CHAPTER ONE

Digital Mapping of Soil Carbon

Budiman Minasny*, Alex B. McBratney, Brendan P. Malone, Ichsani Wheeler

Faculty of Agriculture, Food, and Natural Resources, The University of Sydney, Sydney NSW, Australia
*Corresponding author: budiman.minasny@sydney.edu.au.

Contents

Advances in Agronomy, Volume 118
ISSN 0065-2113, http://dx.doi.org/10.1016/B978-0-12-405942-9.00001-3

Abstract

There is a global demand for soil data and information for food security and global environmental management. There is also great interest in recognizing the soil system as a significant terrestrial sink of carbon. The reliable assessment of soil carbon (C) stocks is of key importance for soil conservation and in mitigation strategies for increased atmospheric carbon. In this article, we review and discuss the recent advances in digital mapping of soil C. The challenge to map carbon is demonstrated with the large variation of soil C concentration at a field, continental, and global scale. This article reviews recent studies in mapping soil C using digital soil mapping approaches. The general activities in digital soil mapping involve collection of a database of soil carbon observations over the area of interest; compilation of relevant covariates (*scorpan* factors) for the area; calibration or training of a spatial prediction function based on the observed dataset; interpolation and/or extrapolation of the prediction function over the whole area; and finally validation using existing or independent datasets. We discuss several relevant aspects in digital mapping: carbon concentration and carbon density, source of data, sampling density and resolution, depth of investigation, map validation, map uncertainty, and environmental covariates. We demonstrate harmonization of soil depths using the equal-area spline and the use of a material coordinate system to take into consideration the varying bulk density due to management practices. Soil C mapping has evolved from 2-D mapping of soil C stock at particular depth ranges to a semi-3-D soil map allowing the estimation of continuous soil C concentration or density with depth. This review then discusses the dynamics of soil C and the consequences for prediction and mapping of soil C change. Finally, we illustrate the prediction of soil carbon change using a semidynamic *scorpan* approach.

1. INTRODUCTION

Soil carbon (C) is recognized as the largest store of terrestrial carbon (Batjes, 1996; Jobbagy and Jackson, 2000; Lal, 2004). Globally, its storage capacity is much larger compared with the pools of carbon in the atmosphere and vegetation. There is now a large and growing interest in knowing the size of soil carbon pool and its sequestration potential. Mapping the spatial distribution of soil carbon has been of great interest as exemplified by the increasing number of publications in mapping soil carbon stock globally and nationally (Grunwald, 2009). This is reflecting the response to the demand for a more accurate assessment of soil carbon pool at a better resolution. Many articles have been published, quantifying and mapping soil carbon storage at the field, landscape, regional, continental, and global scales (Bernoux et al., 2002; Post et al., 1982). Conventional methods that used soil maps as the basis of soil carbon estimates are still being used for mapping areas that have a limited number of soil observations (Batjes, 2008b). However, digital soil mapping technology has progressed rapidly in the past

decade, making it operational for routine mapping over large areas (Bui et al., 2009; Grunwald et al., 2011; Rawlins et al., 2009; Triantafilis and Buchanan, 2010). Digital soil mapping was identified as one of the emerging research fronts in agricultural sciences in the December 2009 issue of the Thompson Reuters Essential Science Indicators[SM1]. Polygon-based soil maps are now being replaced with digital maps of soil carbon content and their associated uncertainties for new areas or previously mapped areas. These maps are stored and manipulated in digital form within a Geographical Information System (GIS) environment, creating the possibility of vast arrays of data for analysis and interpretation (Grunwald, 2009; Meersmans et al., 2009; Mueller and Pierce, 2003; Triantafilis et al., 2009).

This article will review the state of the art in mapping soil carbon and soil carbon change by using digital soil mapping approaches. Mapping and the knowledge of the spatial distribution of soil carbon is useful to

- Provide a baseline carbon level, which can be useful when soil carbon is included in greenhouse gas emissions trading schemes;
- Help localize the variables controlling soil carbon;
- Assist in natural resource management and monitoring;
- Identify potential project locations for soil-based carbon sequestration; and
- Serve as an input into mechanistic simulation models.

There is, in general principles, an essential difference between mapping of soil carbon and accounting of soil carbon. Mapping activity attempts to give an image of the spatial distribution of soil carbon, and while we can use mapping for temporal soil carbon auditing, it will generally be an expensive exercise. In auditing, we are only interested in knowing the total amount of carbon over an area for a particular depth at a particular time, and we do not need to know the exact spatial distribution of carbon. The efficiency of auditing is in the use of statistically design-based sampling strategy (Brus and de Gruijter, 2011). As it is a substantial topic of its own, the issue of auditing will not be discussed here.

2. REVIEW OF PAST STUDIES

2.1. Past Studies

There have been numerous global estimations of soil carbon stocks, and most of them are derived from existing soil maps. The results vary and do

[1] http://sciencewatch.com/dr/erf/2009/09decerf/.

not state the uncertainty of estimates, for example, the reported estimates for global soil organic carbon (SOC) pool in the upper 1-m profile vary from 1220 Pg (Sombroek et al., 1993), 1395 Pg (Post et al., 1982), 1456 Pg (Schlesinger, 1977), 1462–1548 Pg (Batjes, 1996), 1502 Pg (Jobbagy and Jackson, 2000), and 1550 Pg (Lal, 2004). These variable results could be due to the effect of different methods used and also to the variability in spatial and temporal status of the data.

Conventional methods are still being used for the estimation of soil carbon stock for a region or continent; the estimates are based on existing soil maps using soil–landscape and vegetation associations. The resulting maps are usually in the cartographic scale of 1:1,000,000 or coarser, for example, Africa (Henry et al., 2009), Central Africa (Batjes, 2008b), Brazil (Bernoux et al., 2002), and Congo (Schwartz and Namri, 2002). These maps are indeed still useful where there is little soil information for the area. These maps were used by Milne et al. (2007) in the Global Environment Facility Soil Organic Carbon modeling system to map future SOC stock changes in Brazilian Amazon (Cerri et al., 2007), the Indo-Gangetic plains (Bhattacharyya et al., 2007), and Jordan (Al-Adamat et al., 2007).

Since the development of digital soil mapping technologies in the late 1990s, and formalization of the discipline by McBratney et al. (2003), mapping of soil carbon at the field and regional scales has become an area of active research. Table 1.1 summarizes some recent studies of soil carbon concentration and carbon density maps that have been produced using digital soil mapping technology with the *scorpan* model. Here, we only list studies that have used the *scorpan* approach.

The approach of digital soil mapping follows the *scorpan* spatial prediction function:

$$C_x = f(s, c, o, r, p, a, n) + e, \tag{1}$$

where soil carbon C at spatial position x is a function of soil factors (s), climate (c), organisms, which include land use, human effects, and management (o), relief (r), parent materials (p), age or time (a), spatial position (n), and e is the spatially correlated errors. Except for the "time" or "age" factor, most digital soil mapping examples have either explicitly or implicitly used these factors for prediction of soil carbon. However "time" is also an essential factor in soil carbon prediction. Soil carbon observations denoted as "s" on the right-hand side of the equation are

required to calibrate this model. The assumption is also that the observation should cover the whole range variation in covariates, so that the model can be extrapolated to the whole area. The form of f can be a simple linear model to more complicated data-mining tools such as regression trees and random forests (Table 1.1).

2.2. What Do We Learn from These Studies?

The activities conducted by most studies (Table 1.1) are as follows: (i) collection of a database of soil carbon observations over an area of interest; (ii) compilation of relevant covariates for the area; (ii) calibration or training of a spatial prediction function based on the observation dataset; (iii) interpolation and/or extrapolation of the prediction function over the whole area; and (iv) validation based on existing or independent datasets.

A summary of studies cited in Table 1.1 is as follows:

2.2.1. Sources of Data

For field and watershed scale studies, most studies collected soil samples that were guided by environmental covariates. For regional and continental studies, except for France, UK, or nations that have a national monitoring network, most studies were based on legacy soil data.

2.2.2. Extent, Resolution, and Sample Density

Soil carbon has been mapped using digital soil mapping technology at field, regional, national and continental scales with a sampling density from 0.002 to 1100 samples per km^2. Figure 1.1 shows that generally the grid spacing (resolution) of the digital maps increases logarithmically with extent, and the grid spacing decreases logarithmically with sampling density. Although there is no general rule for sample density and grid spacing in digital soil mapping, it also does not mean that we can confidently generate maps at a high resolution using low sampling densities. The uncertainty of prediction should reflect this. Although there are large variations, involving various studies at different depths, the graph shows that the prediction accuracy increases logarithmically with increasing density of observation (Fig. 1.1c).

2.2.3. Depth

Most studies predict soil carbon stock for the top 10–30 cm, and only a few studies have measured carbon stock down to 1 m.

Table 1.1 A review of recent studies on digital mapping of soil carbon

Study area	Extent (km^2)	Maximum depth of prediction (cm)	Grid spacing/ resolution	Number of samples	R^2 prediction	Validation	Covariates	Fitting methods	References
Australia	2,765,000	30	250	11,483	0.41	External	Climate, elevation, lithology, moisture index, soil class	Piecewise linear decision tree	(Bui et al., 2009)
Midwest USA	658,168	50	30	2103		Internal	Terrain attributes, climate, land cover, geology, MODIS NDVI	Geographically weighted regression	(Mishra et al., 2010)
France	543,965	30	12,000	2200	0.91	Internal	Climatic parameters, vegetation NPP, soil properties, and land use	Boosted regression tree	(Martin et al., 2011)
Laos	230,566	100	5	2806	0.42	Internal	Relief, climate, soil map	Cokriging	(Phachomphon et al., 2010)
Agricultural areas, NSW, Australia	158,000	100	250	1145	0.57	Internal	Terrain attributes, climate, land cover, lithology, gamma radiometrics	Piecewise linear decision tree	(Wheeler et al., in press)

Hebei province, China	187,693	100	100	359	0.6	Internal	Terrain attributes, AVHRR NDVI	ANN Regression kriging	(Zhao and Shi, 2010)
Ireland	71,000	10	500	1310		Internal	Rainfall, land cover, soil type	Geographically weighted regression	(Zhang et al., 2011)
Rio de Janeiro State, Brazil	44,000	10	90	431		No	Terrain attributes, Landsat, land cover, lithology	Regression kriging	(Mendonça Santos et al., 2010)
England	18,165	Topsoils	500	5678		No	-	Ordinary kriging	(Rawlins et al., 2011)
Northern Ireland	13,550	20	50	6862		Internal	Gamma K, elevation, soil type	Linear mixed model	(Rawlins et al., 2009)
Southeastern Kenya	13,500	30	1000	95	0.21	Crossvalidation	Climate, topography, vegetation	Regression kriging	(Stoorvogel et al., 2009)
Northern Italy	12,000	30	1000	18,969	0.82	Internal	Soil maps	Regression kriging	(Ungaro et al., 2010)
Flanders, Belgium	10,179	100	15	6900	0.36	No	Land use, soil type, depth to groundwater	Linear model	(Meersmans et al., 2008)
Denmark	5748	20	50	19,836		Internal	Parent material, soil type, topography, NDVI	Classification tree	(Bou Kheir et al., 2010)

Continued

Table 1.1 A review of recent studies on digital mapping of soil carbon—cont'd

Study area	Extent (km^2)	Maximum depth of prediction (cm)	Grid spacing/ resolution	Number of zsamples	R^2 prediction	Validation	Covariates	Fitting methods	References
Edgeroi	1500	100	25	341	0.26	Internal	Terrain attributes, Landsat images	Artificial neural networks (ANN)	(Minasny et al., 2006)
Edgeroi	1500	100	90	341	0.44	Internal	Terrain attributes, gamma radiometrics, Landsat images	Artificial neural networks (ANN) & regression kriging	(Malone et al., 2009)
Peanut basin, Senegal	1030	20	30	155	0.12	External	Geomorphological units, slope position, vegetation,	Expert classification tree	(Mora-Vallejo et al., 2008)
Catchment, Inner Mongolia	3600	100	90	120	0.74	Internal	Land use, geology, soil groups, topography	Random forests	(Wiesmeier et al., 2011)
Santa Fe River Watershed, Florida	3585	30	30	141		No	Landsat image, elevation	Regression kriging	(Vasques et al., 2010a)

Arctic	800	100	15	55	0.56	No	NDVI (ASTER)	Linear model	(Burnham and Sletten, 2010)
Bago-Maragle State Forests, South-eastern Australia	500	100	25	165	0.54	No	Geology, DEM, climate	Linear model	(McKenzie and Ryan, 1999)
Croplands, Luxembourg	420	5	2.6	325	0.89	Internal	Hyperspectral image	Partial least squares (PLS)	(Stevens et al., 2010)
Teramo province, Italy	100	50	40	250	0.7	No	Terrain attributes, Landsat	Regression kriging	(Marchetti et al., 2010)
Drenthe province, the Netherlands	125	90	25	2111	0.46	Independent stratified random sampling	Terrain attributes, groundwater class, land cover, soil type, paleogeography, geomorphology	Linear model	(Kempen et al., 2011)

Continued

Table 1.1 A review of recent studies on digital mapping of soil carbon—cont'd

Study area	Extent (km^2)	Maximum depth of prediction (cm)	Grid spacing/ resolution	Number of samples	R^2 prediction	Validation	Covariates	Fitting methods	References
Dry Creek Experimental Watershed (DCEW), Idaho USA	28	30	30	133	0.62	No	NDVI, potential insolation	Linear model	(Kunkel et al., 2011)
Sedgwick Natural Reserve, Santa Barbara, USA	20.6	A & B Horizons	2	20	0.78	No	Compound topographic index	Linear model	(Gessler et al., 2000)
Eucalyptus plantation, central Madagascar	15.9	30	30	41	0.61	Crossvalidation	Elevation, slope	Boosted regression tree	(Razakamanarivo et al., 2011)
Barro Colorado Island. Panama Canal	15	50	5	165		Crossvalidation	Topographic attributes, soil units, parent material, forest history	Random forests	(Grimm et al., 2008)

Eastern Kentucky	15	30	30	101	0.70	Internal	Landscape position, terrain attributes	Linear model	(Thompson and Kolka, 2005)
IA Watson, Narrabri	4.6	100	5	60	0.80	No	Eca, gamma radiometrics, terrain attributes	Decision tree	(Miklos et al., 2010)
Narrabri	2	10	30	146	0.73	No	Hyperion, Vis–NIR	PLS	(Gomez et al., 2008)
Crisp County, Georgia	1.15	15	2	28	0.98	External	Aerial photograph	Linear model	(Chen et al., 2000)
Wulfen, East Germany	0.7	Surface	6	72	0.9	Internal	Hyperspectral image	Linear model	(Selige et al., 2006)
Kalamazoo County, Michigan, USA	0.5	10	15	78	0.70	No	NIR	Principal component regression	(Huang et al., 2007)
Field 1, Nebraska	0.48	30	4	206	0.46	No	Relative elevation, ECa, and surface reflectance (IKONOS), and soil series	Regression kriging	(Simbahan et al., 2006)
Field 2, Nebraska	0.52	30	4	202	0.66	No	Relative elevation, ECa, and surface reflectance (IKONOS), and soil series	Regression kriging	(Simbahan et al., 2006)

Continued

Table 1.1 A review of recent studies on digital mapping of soil carbon—cont'd

Study area	Extent (km^2)	Maximum depth of prediction (cm)	Grid spacing/ resolution	Number of samples	R^2 prediction	Validation	Covariates	Fitting methods	References
Field 3, Nebraska	0.65	30	4	265	0.75	No	Relative elevation, ECa, and surface reflectance (IKONOS), and soil series	Regression kriging	(Simbahan et al., 2006)
Shiawassee River watershed, Michigan	0.12	20	4	134	0.52	Internal	Terrain attributes	Linear model	(Mueller and Pierce, 2001)
South-eastern Michigan	0.12	10	1	50	0.84	Internal	On-the-go NIR sensor, topography, aerial photograph	Linear model	(Muñoz and Kravchenko, 2011)
Belgian Lorraine region	0.06	5	2.6	68	0.75	Internal	Remotely sensed: Vis, NIR, SWIR (Short Wave Infrared)	PLS	(Bartholomeus et al., 2011)

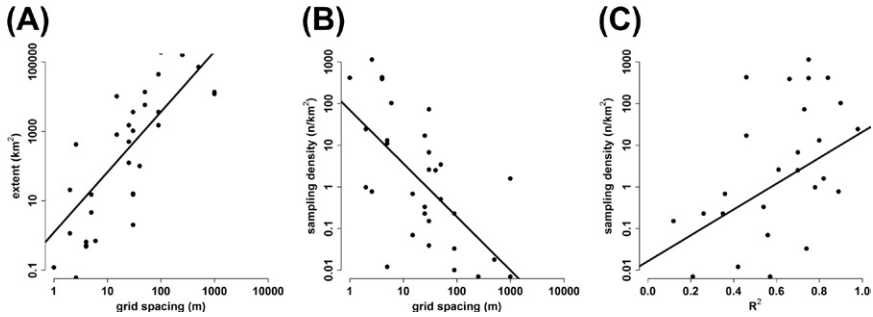

Figure 1.1 Results from previous studies on digital mapping of soil carbon: (a) the relationship between grid spacing (resolution) and extent of the studied areas, (b) the relationship between sample density and resolution of the digital soil maps, (c) the relationship between sample density and the goodness of fit (R^2) for the prediction of soil carbon. For color version of this figure, the reader is referred to the online version of this book.

2.2.4. Validation

Half of the studies do not show any validation, and the other half mostly used crossvalidation and internal validation (random holdback or data splitting).

2.2.5. Uncertainty

Most of the studies do not show any uncertainty of prediction. Only studies based on geostatistical mapping have uncertainty estimates, and most data-mining studies do not show any maps of uncertainty.

2.2.6. Covariates

Topography as manifested through various terrain attributes are generally the most widely used covariates. Land use or land cover and satellite images, (Normalized Difference Vegetation Index (NDVI) derived from remotely sensed images) also play an important role. Gamma radiometrics was also shown to be very useful. For field-scale fine-resolution mapping, remotely and proximally sensed visible to near infrared (NIR) reflectance has been shown to provide good estimates (Muñoz and Kravchenko, 2011).

In the proceeding sections, we will discuss in detail each of these factors and their influence on soil carbon mapping.

3. SOIL CARBON MEASUREMENT AND DEPTH

3.1. Soil Carbon Concentration Versus Density

Total soil carbon is usually separated into SOC and inorganic ($CaCO_3$) carbon. Soil carbon concentration or content can be expressed on a mass basis

by C_m (kg kg^{-1} or percent mass g 100 g^{-1}) or a volume basis by C_v (kg m^{-3}). The relationship between the two is derived from soil bulk density ϱ:

$$C\left(\text{kg C per m}^3\text{soil}\right) = C_m\left(\text{kg kg}^{-1}\right) \times \rho\left(\text{kg m}^{-3}\right). \quad (2)$$

We are usually interested in soil carbon density (C_d) as a measure of the amount of carbon stored; this is expressed as the integral of C_v to a depth z (in meters):

$$C_d = \int_0^Z C_v(z)\, dz, \quad (3)$$

where C_d in kg m^{-2} is the amount of carbon stored per unit land area. Laboratory measurement of total carbon in the soil is usually made by dry combustion, whereas SOC can be made by the wet oxidation method. Recently, visible, near- and midinfrared reflectance spectroscopy has been offered as an alternative, cheaper way to measure soil carbon (Bellon-Maurel and McBratney, 2011; Madari et al., 2006; Morgan et al., 2009; Reeves, 2010; Stevens et al., 2010). The infrared spectroscopy method is based on empirical calibration, where the spectra have been shown to correlate well with total, organic, and inorganic soil carbon contents (Morgan et al., 2009; Vasques et al., 2008). However, the first requirement is the need to establish a database of soil samples where their carbon concentration has been measured using the standard method. The infrared spectra of the soil samples in the library are then related to the standard carbon concentration using empirical functions. The calibration functions can then be used to predict soil carbon concentration for new samples, where only infrared spectra measurement is required (Bellon-Maurel and McBratney, 2011).

Most studies have mapped SOC or total C concentration or density. Because C concentration usually has a positive skewed distribution, most studies used a logarithmic transformation, although square-root transformation sometimes is more appropriate. Some studies have also mapped inorganic C concentration (Miklos et al., 2010; Rawlins et al., 2011) and C fractions, such as recalcitrant C, hydrolyzable C, hot-water-soluble C, and mineralizable C (Vasques et al., 2010b). Other C components maps also have been produced, for example, Carré et al. (2010) mapped the C/N ratio for forest litters in Europe and Angers et al. (2011) mapped the carbon saturation deficit of French agricultural top soils.

3.2. Soil Carbon Variation with Depth

Most studies on soil carbon mapping (Table 1.1) focused on the surface (top 10–30 cm), where soil carbon mostly accumulates. However, the

distribution of carbon at depths (>30 cm) also has an important role. Angers and Eriksen-Hamel (2008) reviewed studies that compared SOC distribution under no-till and full-inversion tillage; they showed that the SOC content was significantly greater under no-till than under inversion in the surface layers. However, at tillage depth and below, the average carbon content can be higher under full tillage than under no till. Meersmans et al. (2009) also pointed out that SOC in the subsoil seems to be strongly related to sorption capacity of pesticides and to denitrification capacity of leached components. Therefore, the knowledge of spatial distribution of soil carbon with depth is of great importance for carbon stock accounting and as inputs to hydrological modeling.

Some studies that examined soil carbon distribution at multiple depths, usually obtained their data from purposive-designed surveys with consistent depth sampling (Grimm et al., 2008; Vasques et al., 2010a). However, soil samples were usually collected based on horizons or fixed depth layers. Studies investigating relationships within legacy soil databases often drew together differing profile sampling approaches, such as sampling by genetic horizons or by varying depth increments, which may also contain samples noncontiguous with depth. Therefore, a soil carbon profile reconstruction method is required to harmonize such data.

Soil carbon has been observed to decline rapidly with depth; the concentration of carbon with depth is usually expressed as an exponential decay function. In one of the early studies, Russell and Moore (1968) found that the organic matter content from 63 profiles from Australia could be expressed as follows:

$$C = C_0 \exp(-kz), \tag{4}$$

where C_0 is the C concentration at the soil surface and k is the rate of decrease, z is depth. They reasoned out that this function is chosen because of its mathematical simplicity and its apparent similarity to the profile depth changes found for biological and related properties.

There are also other equations proposed to describe the decrease of soil carbon with depth, but they are just a variance of the exponential model (Arrouays and Pelissier, 1994; Bernoux et al., 1998; Zinn et al., 2005). Minasny et al. (2006) used a generalized negative exponential depth function:

$$C = C_a \exp(-kz) + C_b, \tag{5}$$

with conditions C_a, C_b, $k \geq 0$, where C is soil C content in volume basis (kg m^{-3}); z is the absolute value of depth from the soil surface (m);

($C_a + C_b$) kg m^{-3} is the C content at the soil surface; C_b is the C content at the bottom of the profile; and k (m^{-1}) is the rate of C decrease with depth.

A disadvantage of using the exponential depth function is that any local variation in the soil profile affects the quality of fit everywhere else in the profile (Webster, 1978). Consequently, they lack flexibility in fitting depth functions, and the quality of fit may be quite varied. Webster (1978) demonstrated that spline interpolators are better for some organic matter profiles of British soils, especially for the Podzols, where the exponential decrease assumption is invalid. Another matter that is usually overlooked is that usually the SOC data are derived from bulked samples taken from particular horizons or layers. It is assumed that the recorded C concentration represents the average value for the depth interval from which the sample was taken. When presented as a soil depth, horizon SOC data should be stepped, whereas soil in general varies continuously with depth. Ponce-Hernandez et al. (1986) proposed a nonparametric depth function, involving a variation of the spline function, called an equal-area spline to model soil attribute depth functions. This approach not only fits the soil C data with depth but it also disaggregates data obtained from horizon bulk samples into a continuous depth distribution. The key characteristics of the equal-area spline are as follows: it consists of a series of local quadratic polynomials with the 'knots' or 'positions of joins' located at the horizon boundaries, and the area of the fitted spline curve is equal to the area of the corresponding layer value, thus ensuring that the mean value of the horizon is maintained. Bishop et al. (1999) tested the ability of equal-area spline to predict soil depth functions based on bulk horizon data of three soil profiles. Their results indicated the superiority of equal-area splines in the prediction of depth functions. Figure 1. 2 shows an example of the equal-area spline fitted to observations of soil carbon from a legacy soil survey data in the Edgeroi area, Australia (Malone et al., 2009). The original samples were collected at various depth intervals; thus, the spline interpolation allowed the harmonization of carbon content at regular depths, which facilitated the prediction of soil carbon content at standard depths.

Breidt et al. (2007) developed a statistical procedure to account for carbon concentration on soil samples collected from varying horizons. They proposed a linear mixed model to estimate the total carbon concentration difference between two tillage systems at the depth of interval of 0–30 cm. The model used parametric fixed effects to represent covariate effects (depth, time, climate), random effects to capture depth correlation, and an

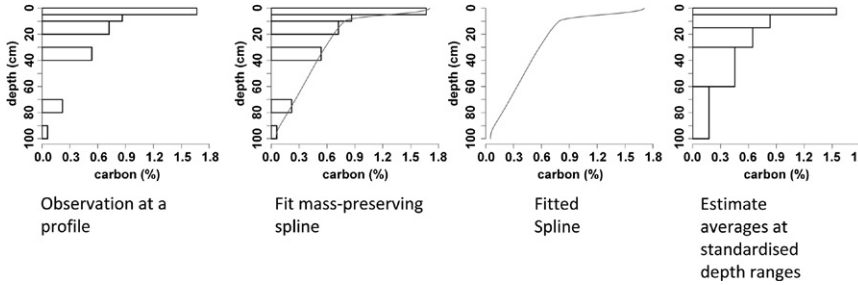

Figure 1.2 An example of equal-area spline fit to soil data and prediction of the soil C content at specified depth intervals. For color version of this figure, the reader is referred to the online version of this book.

integrated smooth function to describe effects of depth. The depth function is specified as penalized splines. The methodology is applied to the problem of estimating a change in carbon stock due to a change in tillage practice from traditional to no-till in the US.

3.3. Another Issue with Depth: The Mass Coordinate System

The calculation of carbon stock (carbon mass over an area) requires the information of soil bulk density. When we use standard depths for comparisons between sites and/or different times, variation in carbon density results can occur due to tillage, compaction, swelling/shrinking, and erosion. This is because the soil mass over certain depths will differ when there is a change in the bulk density, and therefore, comparisons of soil carbon masses in differing soil masses are not appropriate. For example, for two soils sampled to a depth of 10 cm with the same carbon content of 1 g $100\,g^{-1}$, but with bulk densities of 1.0 and 1.3 $Mg\,m^{-2}$, will return soil C masses of 10 and 13 $kg\,m^{-2}$. This difference is due to fluctuating soil masses within sampled depths.

The most popular approach in the soil carbon accounting literature is the equivalent soil mass (ESM) approach (Ellert and Bettany, 1995), which attempts to correct for differences in bulk density by calculating the mass of soil carbon in an ESM per unit area. This is done by first designating the mass of the heaviest soil layer as the equivalent mass. The carbon density from subsequent sampling is then calculated by estimating the thickness of the deepest soil layer required to attain the equivalent mass. The ESM method is quite cumbersome in recognizing the heaviest horizon, and when the boundaries of horizons are not distinct, this is not so simple. Additionally, the depth of the transition between horizons can change

over short distances. This can result in misinterpretation and miscalculation (Lee et al., 2009).

Gifford and Roderick (2003) proposed the use of the mass coordinate system, which is simpler and better for handling this issue. The material coordinate or Lagrange system was proposed in soil science literature by Smiles and Rosenthal (1968) for calculating the water flux in swelling soils. The approach is relatively well known in soil physics and has been applied in the calculation of water flow in swelling soils (McGarry and Malafant, 1987). For carbon accounting, the carbon density estimation can be based on the mass of the soil mineral materials. This is done in the following manner: first, the mineral mass of each sampling layer is calculated from the bulk density ϱ_b (in kg m^{-3}), mineral fraction f_{min} (kg kg^{-1}), and thickness z (m) of the layer:

$$m = z\rho_b f_{min} . \tag{6}$$

The mineral fraction can be estimated from the fraction of the soil that is not organic matter. Next, the cumulative mineral mass for each layer M (in kg m^{-2}) can be calculated from

$$M_i = \sum_{l=1}^{i} m_l. \tag{7}$$

Similarly, the cumulative C density for each layer is also calculated. Afterward, the cumulative carbon density is plotted against the cumulative mineral mass (Fig. 1.3). The amount of carbon for a fixed mineral mass (e.g. 400 kg m^{-2} or 1200 kg m^{-2}) can then be easily calculated. Because we only consider the mineral mass, we exclude carbonates in the calculation. For organic soils, the amount of carbon should be large. In stony soils, we also do not consider materials >2 mm as the mineral mass. Figure 1.3 shows an example of the observations of carbon density that were translated to cumulative mineral mass and cumulative carbon density where the total carbon density to a fixed mineral mass can be readily calculated.

The mass coordinate method is a formal method and has been used for correcting water content changes in swelling soils (McGarry and Malafant, 1987) and for quantifying carbon losses (Smiles, 2009). The assumption is of course that the changes of density are isotropic, the carbon 'moves' together with the mineral material, and that there is no loss or gain of material at the soil surface. The cumulative mass approach should be preferred as the basis for carbon stock accounting and C density reported on a fixed mineral mass per unit area (e.g. see 2006 IPCC Guidelines; Egglestone et al., 2006).

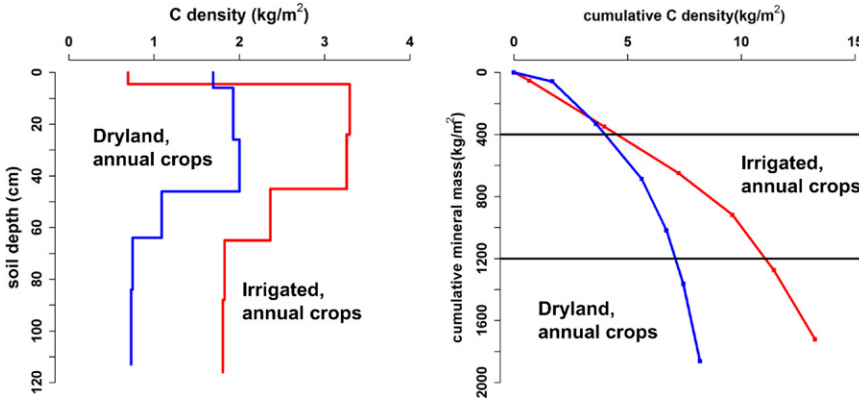

Figure 1.3 An example of the material coordinate system applied to soil carbon observations at 2 sites. Soil carbon densities collected at 6 depth ranges were converted to cumulative mineral mass and cumulative C density. Cumulative C density at specified mineral mass (e.g. 400 and 1200 kg m^{-2}) can be readily calculated. For color version of this figure, the reader is referred to the online version of this book.

4. SOURCE OF DATA: SOIL SAMPLING AND LEGACY DATA

4.1. Sampling in the Presence of Covariates

Here, we only provide a brief review on sampling approaches; a more comprehensive treatise on sampling can be found in De Gruijter et al. (2006). Sampling for carbon mapping can now be done more efficiently with the help of environmental covariates. In the absence of any information, grid sampling or geographical coverage is usually recommended (Walvoort et al., 2010). In the presence of covariates, stratification offers an effective way to cover the variation of soil carbon. The stratification divides an area into strata that are similar in covariate space. Each stratum is then sampled independently, out of which individual sampling units can be selected randomly. Stratified sampling can lead to more efficient statistical estimates (De Gruijter et al., 2006). One way to stratify the area of interest is by using numerical methods or cluster analysis to group the covariates into classes that are similar (Miklos et al., 2010; Simbahan et al., 2006). A fixed number of samples are then taken from each of the classes.

Minasny and McBratney (2006) proposed the use of a conditioned Latin hypercube sampling (cLHS) design to cover the covariate space. They argued that for the purpose of spatial prediction model calibration, it would be beneficial to select samples that cover the whole distribution of values of

each of the covariates. Latin hypercube sampling is a procedure that ensures a full coverage of the range of each variable by maximally stratifying the marginal distribution. The cLHS algorithm attempts to select n observations (sites) from the covariates that can form a Latin hypercube in the feature space. Samples obtained using the cLHS method were found to closely represent the original distribution of the environmental covariates (Brungard and Boettinger, 2010).

4.2. Legacy Soil Data

In many instances (due to constraints in budget and time), legacy soil data are the only source of data available to be used as an estimate of carbon stock baseline at a regional or continental scale. Using legacy soil data can be problematic as the data arise from traditional soil survey. There are no statistical criteria in traditional soil sampling, and this may lead to biases in the areas being sampled. Powers et al. (2011) conducted a meta-analysis of studies that quantified changes in soil carbon stocks with land use in the tropics and found that there is a strong geographical bias of the field observations that were highly unrepresentative of most tropical landscapes. The authors also strongly caution against generalizing average values of land-cover change effects on soil carbon stocks. This study highlighted the problem in using legacy soil data and recommends more representative sampling and monitoring schemes. Bui et al. (2009) meanwhile suggested that the SOC map generated using data-mining techniques based on legacy data, which were collected from traditional survey at different times, still represent a credible map even with a relatively sparse training data. The map produced could be considered as a baseline of SOC content.

Nevertheless, we can assess the reliability and quality of the legacy soil data based on the available covariates. Carré et al. (2007b) used the principle of hypercube sampling to assess the quality of legacy data; they derived a weighing factor of the legacy data based on their coverage in covariate space. First, the covariate space was divided into hypercubes based on the quantiles of the covariate. The occupancy of the legacy data in the hypercube was then checked to determine whether the legacy data occupied the hypercube uniformly or if there was overobservation or underobservation in the partitions of the hypercube. The Carré et al. (2007b) approach also allows the posterior estimation of the apparent probability of sample units being surveyed. This approach also allows the determination of where new sampling units should be located if there is a possibility of sampling investment.

5. PREDICTION AND MAPPING

5.1. Soil Carbon Variation

Soil carbon has a high spatial variation, and a review by McBratney and Pringle (1999) found that the spatial correlation of soil carbon within a field is between 20 and 300 m. This short-range variation is important for field-scale mapping and requires an efficient sampling to capture this variation. The spatial variation of soil carbon also changes with increasing extent, at a continental scale, and the spatial variation can be much larger. Figure 1.4 shows variograms of topsoil organic carbon content in Australia based on a nationwide legacy soil data (McKenzie et al., 2005). The variogram shows a high variation; with increasing variance up to 200 km. Variation in the North–South direction is much higher than the variation in the East–West direction. Overall, there seems to be no apparent "sill" as observed in a field (Fig. 1.4).

At a global scale, the variation of soil carbon can be larger than any regional scale observation; the carbon content fluctuates with latitude and

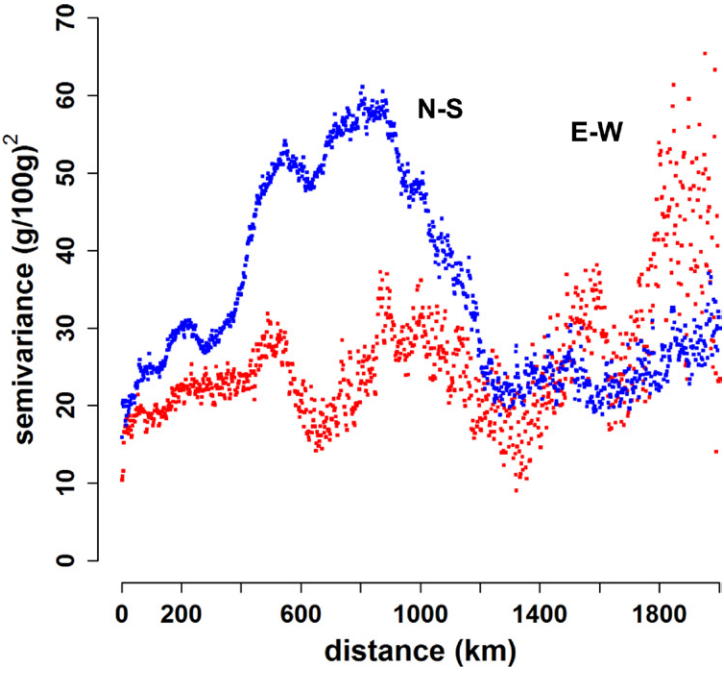

Figure 1.4 Variogram of topsoil organic C in Australia. For color version of this figure, the reader is referred to the online version of this book.

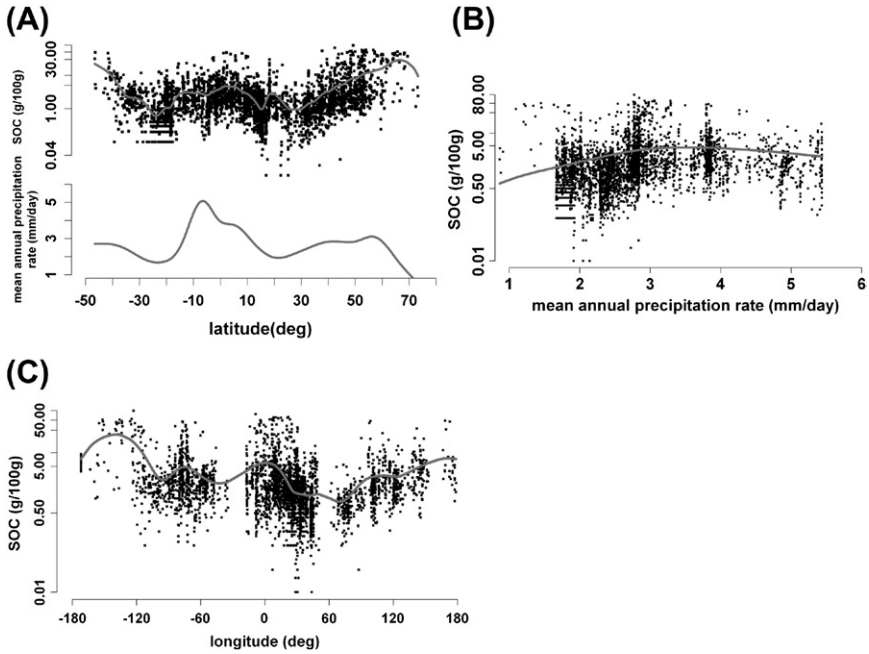

Figure 1.5 (a) The SOC content variation and mean precipitation rate along the latitude. (b) The relationship between mean precipitation rate and SOC. (c) SOC content along the longitude. SOC data from ISRIC–WISE global soil profile dataset (Batjes, 2008a), and the zonally averaged MAP rate is from Adler et al. (2003). For color version of this figure, the reader is referred to the online version of this book.

longitude (Fig. 1.5a, data from ISRIC-WISE global soil profile dataset, Batjes, 2008a). Soil carbon content is greater at higher latitudes, decreases in the midlatitudes, and increases in the tropics. Except for the extreme latitudes, the pattern follows the global mean annual precipitation (MAP)(Adler et al., 2003), where the tropics have a maximum precipitation and a peak around 50 N. The high carbon content at high latitudes corresponds to the low temperature regimes. When we plot the MAP rate along the latitude with soil carbon, we can see that soil carbon tends to increase with the MAP until around 1000 mm, above which the values plateau (Fig. 1.5b), which is also observed by Guo et al. (2006) in the US Soil carbon across the longitude Fig. 1.5c shows the variation over continents, with higher values in the west, and low values around Eastern Africa, and the values increase going toward the east. Figure 1.6 shows the variogram of surface soil carbon content, where the variance can be twice as large as that at the continental scale. The variation is significant, cyclic, and as expected, variation in the north–south

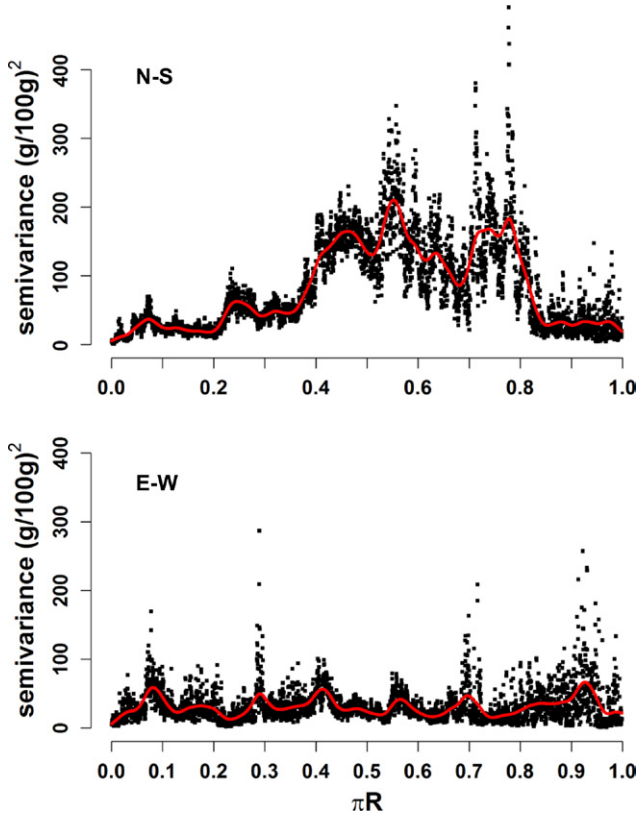

Figure 1.6 Global variogram of the surface soil C content for the north to south and east to west directions; R is the radius of the earth (6378 km). For color version of this figure, the reader is referred to the online version of this book.

direction is much greater than in the east–west direction. The variation in the north–south direction increases at several stages, increasing around 450, 1500, and 2500 km. Meanwhile, there is no clear pattern in the east–west variogram. The premise in digital soil mapping is that the environmental covariates should help in dealing with trends underlying this high variation.

5.2. Environmental Covariates

Jenny et al. (1968) presented one of the first empirical model for carbon which integrated factors of soil formation:

$C = k_0 + k_1$ MAP $+ k_2$ MAT $+ k_3$ parent rock $+ k_4$ slope $+ k_5$ Flora $+ k_6$ Latitude

where k are the empirical coefficients.

The model was calibrated against a moisture transect of 97 surface (0 - 20 cm) soil observations collected across the West Coast of USA ranging from desert to humid region. Jenny found that MAP was the most influential predictor followed by MAT, parent rock, and plant species. As shown in Table 1.1, most studies used elevation and its derivatives to predict soil carbon, and land use/land cover, also important covariates. The covariates are not only useful as empirical predictors, but they should have significant biophysical reasons as drivers of soil C distribution. The covariates can reflect the supply of organic matter to the soil (e.g. net primary productivity) and its potential decomposition (the effect of temperature and moisture). The role of climate becomes important when we look at the global to regional distribution of SOC (see also Fig. 1.5). Global and continental meta-analysis of studies in soil carbon levels after land-use change shows the importance of two critical climate variables: temperature and rainfall (Guo and Gifford, 2002; Powers et al., 2011). Continental scale prediction of soil carbon also revealed the importance of temperature and soil moisture indices as strong predictors (Bui et al., 2009). Bui et al. (2009) found that for topsoil carbon prediction in Australia, climate variables, such as annual mean moisture index, play an important role in delineating SOC zones. This relationship is hypothesized to be associated with plant primary productivity. Other important variables include elevation and lithology.

The study of Bui et al. (2009) also found that the spatial topsoil carbon pattern corresponds well with vegetation, suggesting that the biota drives and regulates the global biogeochemical cycles of elements. They proposed that because the SOC signature still exists from the original native vegetation, and the SOC pattern at the continental scale does not respond quickly to land-use change. This idea is supported by the study of Schulp and Veldkamp (2008), which explored the spatial variability of soil carbon in the Netherlands and found that historical land-use patterns explain a much larger part of the total SOC variability when compared with current land use. Meanwhile, Yang et al. (2007) found that climatic factors explained most of the SOC variation in the top 1 m; however, vegetation type was the stronger predictor when only considering the top 20 cm of the profile. Nevertheless, remotely sensed vegetation parameters (e.g. NDVI) are usually good indicators of primary and ecological productivity, and these data have been successfully used to predict SOC concentration (Bou Kheir et al., 2010; Burnham and Sletten, 2010; Kunkel et al., 2011).

In areas with large terrain variations, soil carbon is often well predicted by terrain attributes (Grimm et al., 2008; McKenzie and Ryan, 1999). Nyssen et al. (2008) working in the Ethiopian Rift Valley suggested that the most important

factor controlling carbon concentration over the studied area was related to the duration of land emergence, which was explained by elevation. The correlation between soil carbon and terrain attributes can also depend on the scale or resolution of interest. For small extent (resolution < 100 m), it is hypothesized that local terrain attributes (slope, aspect, curvatures) are good predictors of soil, where elevation is the driving force behind soil erosion processes. Aspect plays an important role in soil formation, as it creates microclimatic and vegetation differences. However, at resolutions > 100 m, the local terrain attributes become less important, and position in the landscape seems to be more important (the *n* factor of *scorpan*; Arrouays et al., 1995; Moran and Bui, 2002).

Powers et al. (2011) examined studies of soil C change due to land-use conversion in the tropics and noted that, in addition to precipitation, clay mineral composition (in part inherited from parent material) is another important variable that is statistically significant in delineating observations into groups. They classified observations into three groups of clay minerals: allophanic soils dominated by noncrystalline clay minerals that may stabilize soil C, highly weathered soils dominated by low-activity clay with low surface area and cation exchange capacity (CEC), and young to moderately weathered soils dominated by high-activity clay with high surface area and CEC. A very useful covariate that can indicate soil clay content and mineralogy is gamma radiometrics (Wilford, 2011; Wilford and Minty, 2006). Rawlins et al. (2009) found that radiometric K is the most important predictor of soil C in Northern Ireland, especially for organic rich soils. This was because of the good spatial correlation between gamma-ray attenuation and soil moisture, as water reduces the intensity of gamma-rays significantly more than air does. The SOC tends to accumulate in wet or waterlogged areas. Thus, gamma radiometrics is an important covariate for mapping organic soils. In another study in Finland, radiometric K was successfully used in delineating peat areas (Lilja and Nevalainen, 2006).

Remotely sensed visible to NIR reflectance has been shown to be able to map soil carbon over large areas (Bartholomeus et al., 2011; Gomez et al., 2008; Stevens et al., 2010). However, the challenge is of course to be able to remove the influence of vegetation cover from the spectra (Ouerghemmi et al., 2011). Groundwork has shown the feasibility of predicting soil properties using airborne hyperspectral data in areas with bare soil cover. Further, the prediction at areas with bare soil can be extrapolated to the whole field using geostatistical procedures (Lagacherie et al., 2012). At a field-scale, proximally sensed infrared spectra have also been used successfully to map soil carbon (Bartholomeus et al., 2011; Muñoz and Kravchenko, 2011).

In summary, the relationship between environmental covariates and soil carbon depends on the environmental conditions, resolution, and the extent of the study area see (Fig. 1.1). At the continental to regional scale, climate seems to be the most important driving factor: mainly rainfall and temperature. Soil clay mineralogy seems to be a significant driving factor. Gamma radiometrics have been found to be important predictors for carbon at various scales, because of the good correlation between gamma-ray attenuation with soil moisture and clay type. Native vegetation was suggested to present an important signature of carbon at regional scales. In the landscape scale, erosion and deposition also plays an important role. At farm scales, current land-use practices become an important controlling driver. Nevertheless, all these relationships can vary depending on the soil characteristics and their environment. With regards to the use of contemporary climate as a predictor Jenny (1980) wrote: "The computer's verdict of tangible linkages of soil properties to the state factors pertains to today's environment. Either the pedologically effective climate has been stable for a long time, or past climates are highly correlated with modern ones, or the chosen properties have readjusted themselves to today's precipitation."

5.3. Estimating Bulk Density

Carbon stock (the mass of carbon over a unit area) is the preferred currency in soil carbon mapping, as the total mass of carbon within an area can be calculated directly. Thus, bulk density is needed; however, most legacy soil data do not have a measurement of soil bulk density, which therefore needs to be predicted. Tranter et al. (2009) proposed the following model for the prediction of bulk density:

$$\rho_b = \rho_m + \Delta\rho + \varepsilon, \tag{8}$$

where ϱ_b is the soil bulk density, ϱ_m is the typical mineral soil bulk density $\approx f$ (particle size distribution, depth), $\Delta\varrho$ is the variation associated with structural component $\approx f$ (organic carbon, tillage, etc.), and ε is the residual variation. The predicted bulk density for ϱ_m can be considered to be a typical value for a soil with a given particle size distribution, depth, and average structural features. The typical equation for mineral bulk density is usually in the form of

$$\rho_m = a + b\ \text{sand}\ + c\ \text{sand}^2 + d\log(\text{depth}), \tag{9}$$

where a, b, c, d are empirical parameters. This function is defined such that bulk density increases with increasing sand content in a quadratic manner and also increases exponentially with depth as a result of overburden pressure. The $\Delta\varrho$ component is introduced to account for bulk density variation as a function

of soil carbon change. A simple model was proposed by Stewart et al. (1970) and Adams (1973) relating mineral bulk density and organic matter content:

$$\rho_b = \frac{100}{\frac{\mathrm{OM}\,\%}{\rho_{\mathrm{OM}}} + \frac{(100 - \mathrm{OM}\,\%)}{\rho_{\mathrm{m}}}}, \tag{10}$$

where OM% is organic matter percentage, and ϱ_{OM} is organic matter bulk density = 0.224 g cm^{-3}. This model merely shows an increase in specific volume of 0.06 cm^3/g with a 1% increase in soil carbon concentration. These relationships (Eqns (9) and (10)) were found to fit well for data from Australia (Tranter et al., 2007), Europe (Hollis et al., 2012), and the tropics (Minasny and Hartemink, 2011). The advantage of using the above relationship is that the mineral bulk density can be defined for each soil type (Hollis et al., 2012), and the variation of soil carbon can be incorporated independently. Some publications, for example, Moreira et al. (2009) suggested that bulk density can be predicted from infrared spectroscopy. We would be cautious of such a relationship, although in principle spectral calibration is a type of pedotransfer function, we cannot infer the physical relationships as demonstrated above.

5.4. Mapping Soil Depth Function

Most soil carbon mapping is performed in 2-D, where carbon concentration or stock is mapped for a prescribed depth interval. However, it would be beneficial if we could map the carbon content as a continuous function of depth, as soil carbon stock can be readily calculated at any depth. In an unpublished presentation, Barson et al. (2004) compiled a database of soil profiles to estimate the size of the Australian soil carbon pool. A linearized version of a negative exponential depth model was fitted to the profile SOC data. The parameters of the exponential model were then predicted by using environmental variables. These predictive equations were combined with continental surfaces for bulk density, clay content, pH, elevation, and climatic parameters to predict SOC stored at different depth across the Australian continent at a grid spacing of 5 km.

Minasny et al. (2006) used the negative exponential depth function (Eqn (5)) to describe soil carbon concentration variation with depth in the Edgeroi area, Australia. They then mapped the parameters of the exponential function using a modified neural network approach, where the functions were calibrated to predict all the parameters simultaneously and to fit the soil C concentration. This approach takes care of the parameter correlation. They predicted parameters of the exponential function (Eqn (5)) over the

whole area, which enabled them to calculate the C distribution over the profile and also the storage of C at any depth. In effect, this creates a pseudo-3-D soil carbon map.

Following this work, Mishra et al. (2009) fitted an exponential function to soil profile data from Indiana, US, and then interpolated the parameters independently using ordinary kriging. A better solution is to interpolate the parameters simultaneously using cokriging (Webster and Oliver, 2007). The procedure in cokriging is slightly more complicated, and mapping them in large areas with sparse observations tends to oversmooth the reality. Meersmans et al. (2009), unaware of the previous works, developed empirical functions that predicted the parameters of the exponential depth function for the area of Flanders in Belgium. The functions were stratified based on land use, and the parameters were related to particle size distribution and height of groundwater.

Realizing the limitation of the exponential depth function, Malone et al. (2009) fitted an equal-area spline function to the soil profile data (Section 3.2). Parameters of the spline function were then interpolated or predicted for the whole area. Following this work, Kempen et al. (2011) developed a method for mapping depth functions based on pedological knowledge combined with geostatistical modeling. Their approach is useful in areas, such as the Netherlands, where soil properties do not vary smoothly with depth, because of anthropogenic or geologic disturbance. They modeled the distribution of soil organic matter content for each of the typical soil horizons. Five depth function building blocks were defined, and for each soil type, the depth function structure was obtained by stacking a subset of model horizons. The parameters of the depth function for each of the horizons were interpolated using a geostatistical procedure.

Although we can model the distribution of carbon with depth, generally, the prediction accuracy decreases with depth (Kempen et al., 2011; Minasny et al., 2006; Wheeler et al., in press). This indicates that the environmental covariates mainly explain the soil conditions in the top 30–50 cm. The environmental covariates seem to have lost their elucidation power in the lower parts of the profile (Vasques et al., 2010a). The challenge remains to find potent covariates that can explain subsurface soil variation.

5.5. Global Mapping of Soil Carbon

The most widely used global map of soil carbon is based on the 1:5 million map produced by the Food and Agricultural Organization (FAO) and United Nations Educational, Scientific and Cultural Organization

(UNESCO) in 1981. In the mid-1990s, a 9-km raster version was produced by the FAO. The digitized FAO–UNESCO map is still widely used for global studies on such topics as climate change, world food production, and environmental impact assessment (Batjes, 1996). There are also more recent global maps of the SOC, including SOC density up to a 1-m depth at a resolution of 1 km (Scharlemann et al. 2009). The IPCC (Intergovernmental Panel on Climate Change) released a global above- and below-ground biomass carbon density that was rasterized to a resolution of approximately 1 km (Ruesch and Gibbs, 2008).

GlobalSoilMap.net is a new project developed by a consortium, which aims to create a digital map of the world's soil properties. This global effort will provide access to the best available map of soil properties across the globe at a resolution (grid spacing) of 3 arc second (~90 m) along with its confidence of prediction in a consistent format at the depth ranges of: 0–5, 5–15, 15–30, 30–60, 60–100, and 100–200 cm. Soil carbon concentration is one of the key properties that will be mapped.

Realizing that it is a significant effort to apply the *scorpan* prediction function across the globe, the approach taken (for global soil mapping) is a pragmatic one (Minasny and McBratney, 2010). The methods that are used (or will be used) for mapping consider the nature, availability, and density of existing legacy soil data. Figure 1.7 shows a first approach of mapping soil carbon in the USA based on a 1:250,000 soil map from the USDA–NRCS (United States Department of Agriculture - Natural Resources Conservation Service), where the soil polygons were converted to raster (resolution 90 m) estimates of organic carbon content (based on the STATSGO2 database) for the 6 depth intervals of the GlobalSoilMap.net specification. Currently, this effort is mirrored elsewhere in the globe.

5.6. A Regional Example

Here, we present an example of a pseudo-3-D soil carbon mapping in the Edgeroi area of Australia (Malone et al., 2009). This area of 1500 km^2 was covered by 341 soil profile observations, from which 210 are arranged on a systematic, equilateral triangular grid with an approximately 2.8-km spacing between sites, and 131 are distributed more irregularly or on transects. Soil samples were taken from the profiles at depths: 0–0.1, 0.1–0.2, 0.3–0.4, 0.7–0.8, 1.2–1.3, and 2.5–2.6 m, from which the soil physical and chemical analyses were conducted. SOC concentration and density were mapped at a grid spacing of 90 m on point support using various environmental covariates (digital elevation model and its derivatives, Landsat TM images, and

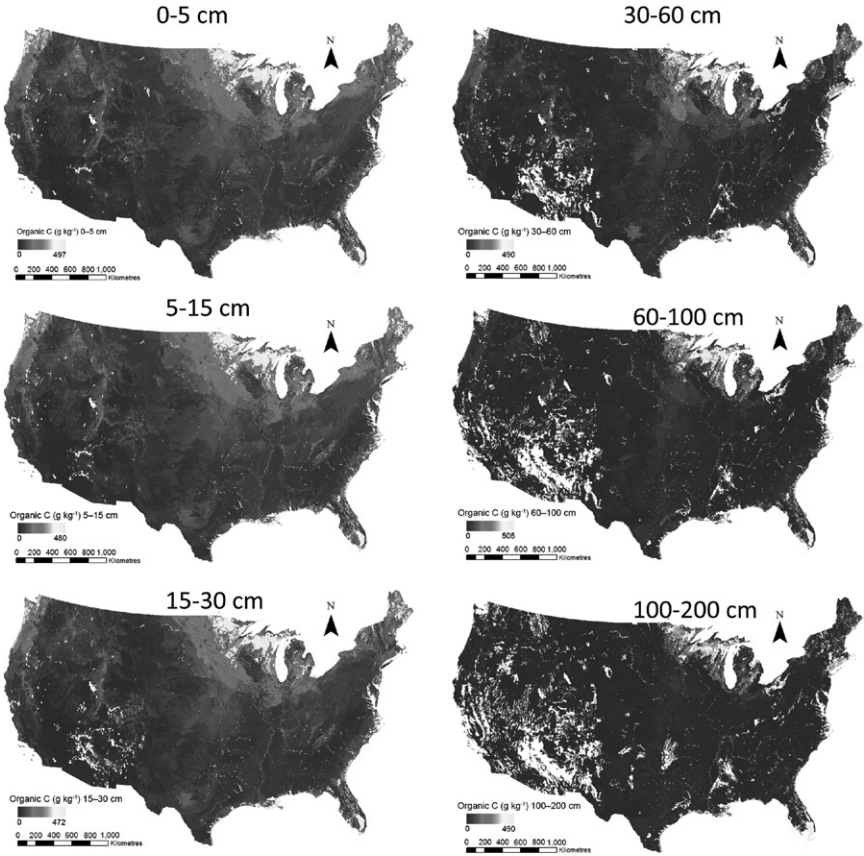

Figure 1.7 Map of soil carbon in North America at 6 depths based on GlobalSoilMap.net specifications. For color version of this figure, the reader is referred to the online version of this book. (*Figure courtesy of Nathan Odgers & Jon Hempel, USDA–NRCS.*)

gamma radiometrics) as predictors. The steps taken to produce the SOC maps were as follows:

- Compiling the soil observation data and relevant environmental covariates;
- Calculation of bulk density using pedotransfer functions (Tranter et al., 2007);
- Calculation of the SOC on volume basis (kg m^{-3}) using predicted bulk density;
- Fitting of the equal-area spline to the SOC and bulk density profile data;
- Joining the observation and covariates to form a calibration dataset;
- Deriving spatial prediction models from the calibration dataset to predict parameters of the depth function for the SOC and bulk density from environmental covariates;

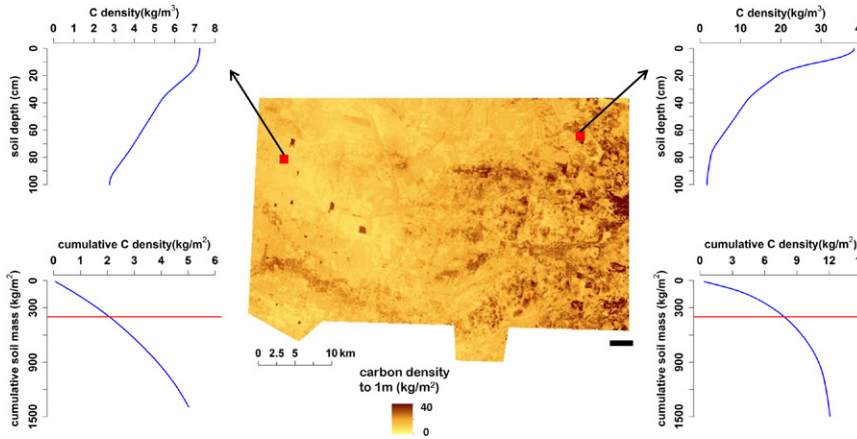

Figure 1.8 Map of soil carbon stock in Edgeroi, Australia. The semi 3-D approach allows the estimation of continuous depth of soil carbon density; based on a map of the bulk density, the total C density at any cumulative mineral mass can be readily calculated. For color version of this figure, the reader is referred to the online version of this book.

- Using the generated spatial prediction models to map the whole area for the SOC content and bulk density; and
- Calculating the uncertainty of the prediction (Malone et al., 2011).

The approach here mapped the SOC on volume basis and bulk density, as we can derive soil carbon density to any depth by integrating the SOC on volume basis. Using the mass coordinate approach, the cumulative soil mass and cumulative C density can be easily calculated see (Fig. 1.8). Figure 1.9 shows that by mapping the continuous function of carbon across the area, we can make nonlinear queries that cannot be done easily using conventional approaches, for example, the calculation of the depth at which cumulative mineral soil mass = 400 kg m^{-2} and the corresponding cumulative C density.

6. UNCERTAINTY AND VALIDATION

6.1. Uncertainty

An important output of digital soil mapping product is the availability of an uncertainty or measure of confidence in prediction. However, most of the studies (Table 1.1) do not show any uncertainty of prediction even though they are critical in determining the prediction confidence (Goidts et al., 2009). Unless the method is based on geostatistical studies, most data-mining studies do not show any estimates of uncertainty. Statistical methods for uncertainty analysis include but are not limited to Monte Carlo

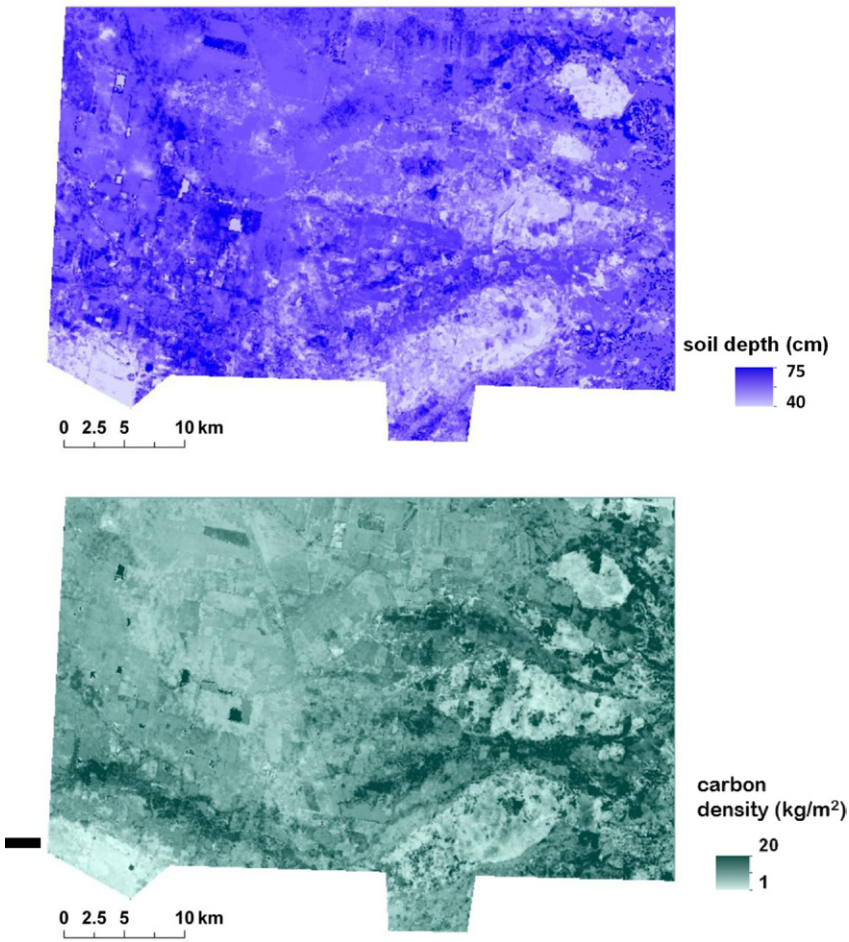

Figure 1.9 Mapping soil with a continuous depth function allows for nonlinear queries, such as (a) the depth at which cumulative mineral soil mass = 400 kg m^{-2} and (b) their corresponding cumulative C density. For color version of this figure, the reader is referred to the online version of this book.

simulation, bootstrapping, or Bayesian approach. Uncertainty analysis also allows the identification of the main source of error in the prediction. This is illustrated in the study of Goidts et al. (2009) who used an error propagation method to quantify the relative contribution of each of the variables and their interaction involved in estimating the SOC stock (SOC concentration, sampling depth, bulk density, and rock fragment content). They found that the main sources of uncertainty are the variability of the SOC concentration (due to errors from the laboratory and spatial variability) and of rock fragment content.

In a mapping study, Meersmans et al. (2009) calculated the parameter uncertainty of the exponential depth function using a Monte Carlo simulation. For mapping large areas, Monte Carlo simulation and the Bayesian approaches can be computationally too expensive as they require maps to be generated for each of the realizations (in the order of 1000–10,000 simulations). Malone et al. (2011) proposed the use of an empirical approach to derive the estimates of uncertainty. Uncertainty in this case is treated as the probability distribution of the output model errors, which comprises all types of uncertainty (model structure, model parameters, and data). This is particularly useful when we are dealing with data-mining tools in combination with the regression-kriging approach, where it is difficult and impossible to derive an analytical model for the parameter uncertainty. The idea behind this approach is to partition the model input (covariates) space into different clusters having similar values of model errors. The covariates used for prediction is partitioned into several classes using the fuzzy k-means with extragrades algorithm (McBratney and De Gruijter, 1992). Each class is then represented by a prediction interval determined from the empirical distribution. The fuzzy k-means with extragrades method is also used to identify and sufficiently penalize those observations outside the domain of the calibration data. Using the class centroids, a new observation can be allocated memberships to each of the established classes. Prediction limits for new observations then can be calculated as a weighted average of the membership values.

6.2. Validation

Half of the studies on soil carbon mapping (Table 1.1) do not show any validation. The other half of the studies used internal validation using random holdback. Validation of soil maps can be done in different ways:

- Crossvalidation, which can be leave-one-out or n-fold crossvalidation (Efron and Tibshirani, 1994). In leave-one-out crossvalidation, a sample point is left out, whereas the rest is used to calibrate the prediction model; the left-out sample is used to assess the accuracy of the calibrated model. The process is repeated for all samples. Meanwhile, in n-fold crossvalidation, the dataset is divided into n section or fold, and the crossvalidation process is repeated for n-folds.
- Internal validation using data splitting or random holdback, where a portion of the data (usually 30%) are randomly held back and excluded from model calibration. These holdback data are used to check the accuracy of the model.
- Independent sampling, where additional samples or observations are collected to check the accuracy of the model.

As explained by Brus et al. (2011), crossvalidation and random holdback may not provide unbiased estimates of map accuracy because of the nature of the data used. The prediction errors will generally be spatially correlated, and the data itself can be biased. Thus, they recommended the use of a probability sampling scheme to collect additional samples that can provide an unbiased quality measure of the map. Because of the high expense of resampling, only few studies (e.g. Brus et al. (2011) and Kempen et al. (2011)) have afforded independent sampling for the validation of soil C maps using a stratified simple random sampling approach.

7. MAPPING AND PREDICTING SOIL CARBON CHANGE

7.1. Mapping Soil Carbon Change

Mapping soil carbon change over an area can be done properly for areas with a monitoring scheme (Martin et al., 2011). Spatiotemporal models can only be applied in an area with a proper monitoring network. For example, Bellamy et al. (2005) used data from the National Soil Inventory of England and Wales obtained between 1978 and 2003 to show that carbon was lost from soils across England and Wales over the survey period at a mean rate of 0.6% yr^{-1}. Soil carbon change can also be mapped in countries having a comprehensive national scale database of soil carbon concentration sampled at different times (Meersmans et al., 2010). Fantappiè et al. (in press) used a database of Italian soils to map the SOC content between two periods (1979–1990 and 1991–2009) and showed that climate change generally had a small influence on SOC variations.

Legacy soil data collected at uneven space and time intervals can sometimes be used to indicate temporal changes. Lindert (2000) compiled a database of topsoil properties from Indonesia, which were collected from 1930 to 1990. Using regression models, he showed the decline in soil organic matter and N content with time in Java and the increase in total phosphorus and potassium. This work was criticized by soil scientists, as the soil test results came from various places at various times, which create problems such as possible systematic bias due to unrepresentative repeated sampling, change in sampling depth, and/or change in analytical method over time (Dobermann, 2002). Nevertheless, recent work in France has shown that a nationwide soil test database, which was collected for soil fertility assessment, can be used to detect decadal spatiotemporal changes in soil carbon (Saby et al., 2008). Minasny et al. (2010) used legacy soil data of the SOC in Java collected by the Indonesian Center for Agricultural Land Resources & Development

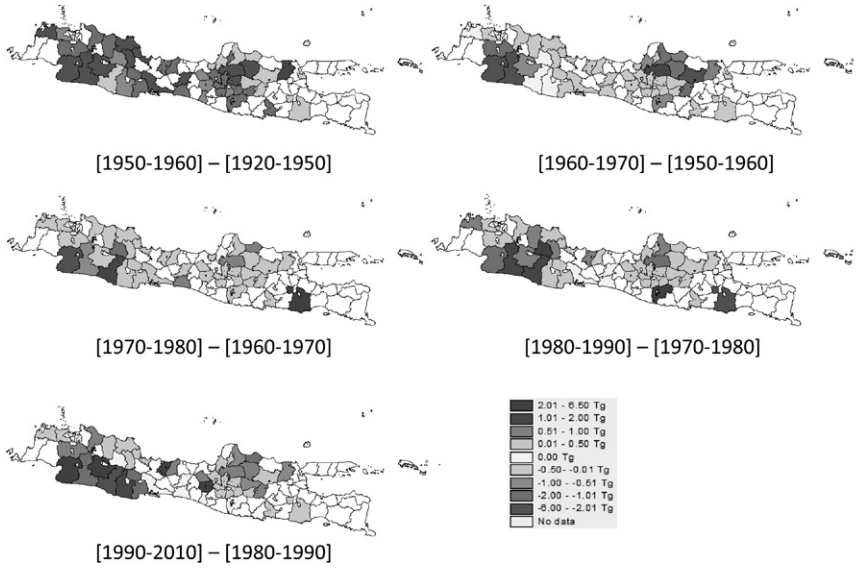

Figure 1.10 The changes in the C stock over successive periods for the top 10-cm soil in Java, Indonesia. Data based on Sulaeman et al. (2010). For color version of this figure, the reader is referred to the online version of this book.

from 1923 to 2007. They aggregated the data into spatial administrative entities as most of the data do not have proper geographical coordinates, and mapped the changes in topsoil carbon content per decade (Sulaeman et al., 2010). Spatial analysis (Fig. 1.10) showed the trend of the SOC over the island with an apparent decline of the SOC concentration from around 2% in 1930–1940 to 0.7% in 1960–1970. However, there is an increase in the SOC content after 1970, with a median level of 1.1% in the 2000.

The variation of the soil C over time also has another implication that we can only use data from the relevant period for digital soil mapping. An alternative will be to standardize the C level collected at various times to a common period. A simple way is by adjusting the mean of the data at various periods to a desired period. A more elaborative option is to run a dynamic simulation model and predict the likely soil carbon at a common time.

7.2. Predicting Soil Carbon Change

Digital soil mapping only maps soil carbon status at a particular time; however, we can use the map to predict the likely carbon change. There are two ways we can approach this:

(1) Dynamic–mechanistic simulation model

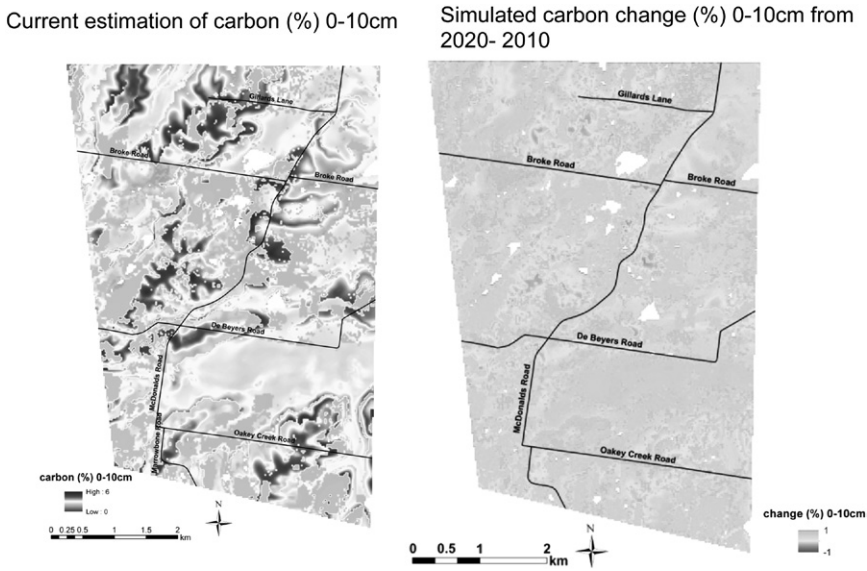

Figure 1.11 Predicted soil organic C content 0–10 cm for an area in the Hunter Valley, and simulated changes with land-use change. For color version of this figure, the reader is referred to the online version of this book.

The map of SOC can be fed into a dynamic–mechanistic simulation model. Most SOC simulation models do not consider a spatial aspect. Although there is work that incorporate SOC models into a GIS environment (e.g. Huber et al., 2002), the models still run as a one-dimensional component with no spatial connection (Tonitto et al., 2010). The SOC model is executed individually at each pixel based on the likely scenario, for example, increased temperature, or change in land management or land use (C input). This is the most widely used approach as indicated by a meta-study by Grunwald (2009). Landscape information can be incorporated by including a spatial process, for example, erosion and deposition. This is demonstrated by Walter et al. (2003) who performed field-scale simulations of the spatiotemporal evolution of topsoil organic C at the landscape scale over a few decades and under different management strategies. Figure 1.11 shows an SOC concentration map at 0–10 cm of an area in the Hunter Valley, Australia, which was generated using a digital soil mapping approach. We used this map for a scenario modeling, where the current vineyards are no longer profitable and may be changed to pasture. Using a simple 2-compartment model (Hénin and Dupuis, 1945), we estimated the SOC change for the next 10 years:

$$\mathrm{d}C/\mathrm{d}t = hI - kC\,, \tag{11}$$

where dC/dt represents the change in the SOC over time, and I is the annual C input, h is the isohumic coefficient, and k is the decomposition constant. The value of parameters h and k depend on the type of organic matter, soil type, temperature, and other environmental variables. Some values are suggested in the literature (e.g. Andriulo et al., 1999). The mean SOC level for this area in 2010 is 2.9 g $100\,g^{-1}$ and the estimated SOC level in 2020 is 3.3 g $100\,g^{-1}$. Using this rudimentary approach, we can identify areas suitable for carbon sequestration and can estimate its carbon sequestration potential.

As most soil carbon dynamic models do not have a spatial component, and only simulate topsoil condition, Viaud et al. (2010) suggested a landscape-scale modeling approach to take into account the transfer and transformation processes in the SOC of a landscape. They proposed the design of a three-dimensional, spatially explicit representation of the landscape system with the integration of functional interactions and organic matter transfer functions into the conventional SOC modeling framework. Rudimentary landscape models of SOC dynamics as a component of long-term soil genesis models have been presented by Minasny et al. (2008) and Yoo et al. (2006). A spatial carbon model that includes production and input (I), decomposition (k), vertical mixing/bioturbation (q_m), and gains and losses (q_a and q_l) can be expressed as follows:

$$dC/dt = I - kC + q_m + (q_a - q_l)\,. \tag{12}$$

The availability of such a model should help us make a better prediction of the soil C change in a landscape or region. Nevertheless, currently, there is still a disconnection between soil C mapping and mechanistic C dynamics modeling (Walter et al., 2006).

(2) Static-empirical model

The scorpan approach can also be used to infer the likely changes in soil properties over time as discussed in McBratney et al. (2003) termed 'partially dynamic soil scenario maps.' This advantage has not been explored yet; if we know any of the changes of the *scorpan* factor over time, we can project the existing soil map forward Δt. For example, a change in the temperature due to climate change can be projected onto a *scorpan* model by calculating $c + (\Delta c/\Delta t)$ for all points in the map and running the prediction function. Similarly, for land-use change, we can infer the C change by calculating the change in the o factor: $o + (\Delta o/\Delta t)$. The C level at Δt can be calculated as follows:

$$C_{t+\Delta t} = C_t + \Delta c/\Delta t + \Delta o/\Delta t\,.$$

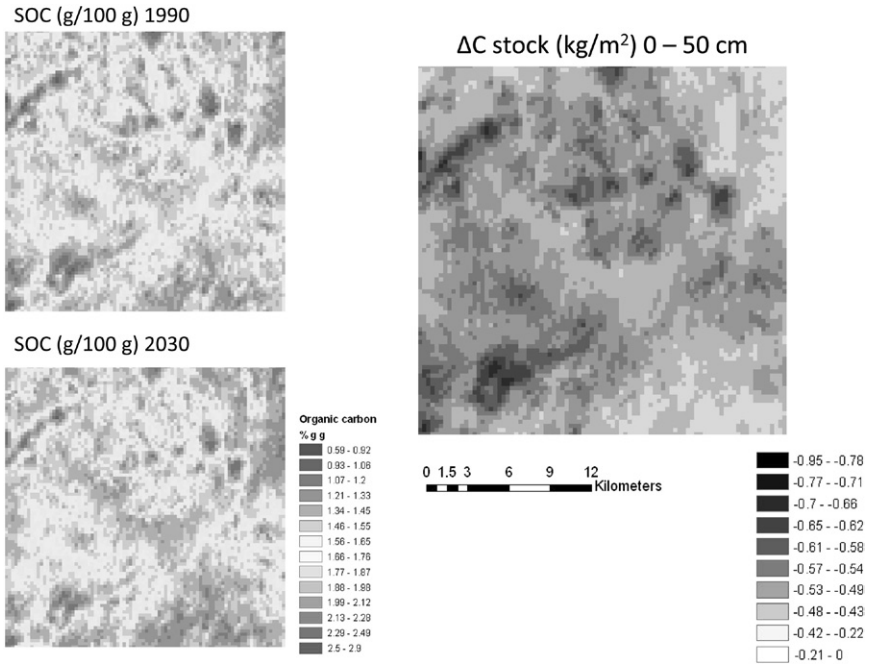

Figure 1.12 Map of the SOC at 0–50 cm in the southern part of NSW. The 1990 map was generated using a rule-based model based on legacy soil data and environmental covariates. The C level in 2030 was estimated under a likely climate change scenario (increase in the MAT and decrease in the MAP). The rule-based model was recalculated to reflect the climate change, and a map of likely C status in 2030 was produced. The change in carbon stock was then calculated based on estimates of the bulk density. For color version of this figure, the reader is referred to the online version of this book.

We demonstrate this approach by showing an example of projecting the influence of climate change on soil C level in a region of New South Wales (NSW), Australia. The baseline SOC concentration map (0–50 cm) was derived using legacy soil data collected in a nationwide database (McKenzie et al., 2003). A map was derived using a rule-based model based on the legacy data and environmental covariates with a grid spacing of 250 m (Wheeler et al., in press). Climate information was found to be important predictors in the spatial prediction model. See Wheeler et al. (in press) for the techniques involved in the mapping. We focused on an area of 49,000 ha in the southern part of NSW (Fig. 1.12) and estimated the likely change in soil carbon with climate change. We used the 50th percentile of the estimated likely change in the mean annual temperature (MAT) and MAP by 2030 (relative to 1990 levels) for the corresponding area of

NSW (Watterson et al., 2007). For a high emissions scenario, the MAT is expected to increase 0.6–1 °C (average 0.8 °C) and MAP to decrease 2–5% (average −3.5%). Using this information, we adjusted the climate covariates and recalculated the SOC concentration from the rule-based model. The assumption in this case is that the C level is at a steady-state condition (amount of input is constant). The projected map shows that there is an average potential loss of 5 t of C per hectare. Such information will help decision makers to decide on alternative land-management techniques that could reduce this loss.

This empirical approach is a relatively quick and pragmatic way to produce a first-cut scenario to predict the change in soil C. It has limitations compared with a dynamic simulation model, such as lack of feedback and possible extrapolation problems. Nevertheless, the *scorpan* approach has been locally calibrated, and any changes in the factors should reflect the changes in the predicted C.

Grunwald et al. (2011) recently proposed a space–time modeling framework (soil, topography, ecological and geographic properties–atmospheric, water, biotic, and human; STEP-AWBH), which attempts to incorporate anthropogenic factors to predict soil properties of the future. In their approach, the soil prediction function is estimated from various spatially explicit environmental variables, which can be grouped into 2 classes: STEP (parent material and geologic properties) factors that tend to be static within a human time frame and is thus represented in the model at one time, AWBH factors account for space and time, whereby the time component may be aggregated to represent different time vectors. Each of the AWBH factors can be represented by various covariates, such as climate, soil moisture, land use.

8. CONCLUSIONS

Digital soil mapping has taken off in the past decade, thanks to the advances in computing, spatial databases management, and numerical modeling. Digital mapping of soil carbon has quickly moved from a research stage to being operational with maps of carbon concentration and carbon stock being produced at various places in the world from field to regional and continental scale and extent. The *scorpan* spatial soil prediction function has been used to different extents and resolutions. Mapping has also evolved from a simple 2-D map to a pseudo-3-D representation.

From this review, we outline several important points that need to be considered to advance the art and science of mapping soil carbon:

- Obtaining representative soil samples for spatial modeling is important. The soil–landscape relationships built using the *scorpan* model only describes the empirical correlation found from the data. Biased samples will also make the model biased toward the observations.
- Digital maps produced using the *scorpan* approach mostly will reflect the covariates. If the covariates are poor, then the resulting map will also show numerous artifacts and their associated inadequacies.
- The various scales of covariates, the relationship between soil observation and covariates can change with the scale of the covariates. In some cases, covariates at a larger scale can be more useful than at a detailed fine resolution. There is still a need for more work to examine the spatial decomposition of covariates (Mendonça-Santos et al., 2006).
- The dynamics of soil carbon with time means that we need to consider the time dimension in our maps. Questions were raised on how to use and to standardize legacy data collected at different times? The integration of digital soil mapping and mechanistic soil–landscape modeling will help solve this problem.
- Mapping and estimating change: digital soil mapping should be able to provide a semidynamic model to estimate how soil carbon will change when one or several of the *scorpan* factors evolve with time.
- Models incorporating the mechanistic simulation model for spatial prediction can enhance our understanding of soil carbon distribution. As we have learned from empirical studies, the covariates used by data-mining models can infer the biophysical drivers of soil carbon distribution. However, we can also use our dynamic understanding of the soil–landscape system to better understand and predict the distribution and changes. We should be able to use a more mechanistic and dynamical relationship analyzing the spatial (and temporal) carbon data. This work will present a dynamic representation of soil carbon where digital soil assessment can be easily incorporated.
- There is still very little forward looking on digital soil carbon assessment (Carré et al., 2007a). The maps of soil carbon have not been taken further for the assessments of soil functions and threats.
- A global map of soil carbon at a fine resolution with a consistent specification will help provide more information to decision makers, and modelers, and provide a better estimation of current carbon stock and distribution.

ACKNOWLEDGMENTS

Budiman Minasny acknowledges the ARC QEII fellowship received from an ARC Discovery Project. This work is also part of an ARC Linkage project "The auditability of soil carbon." The authors thank Jon Hempel and Nathan Odgers, USDA–NRCS, for use of the US soil carbon map.

REFERENCES

Adams, W.A., 1973. The effect of organic matter on the bulk and true densities of some uncultivated podzolic soils. J. Soil Sci. 24, 10–17.

Al-Adamat, R., Rawajfih, Z., Easter, M., Paustian, K., Coleman, K., Milne, E., Falloon, P., Powlson, D.S., Batjes, N.H., 2007. Predicted soil organic carbon stocks and changes in Jordan between 2000 and 2030 made using the GEFSOC modelling system. Agric. Ecosyst. Environ. 122, 35–45.

Andriulo, A., Mary, B., Guerif, J., 1999. Modelling soil carbon dynamics with various cropping sequences on the rolling pampas. Agronomie 19, 365–377.

Angers, D.A., Arrouays, D., Saby, N.P.A., Walter, C., 2011. Estimating and mapping the carbon saturation deficit of French agricultural topsoils. Soil Use Manage. 27, 448–452.

Angers, D.A., Eriksen-Hamel, N.S., 2008. Full-inversion tillage and organic carbon distribution in soil profiles: a meta-analysis. Soil. Sci. Soc. Am. J. 72, 1370–1374.

Arrouays, D., Pelissier, P., 1994. Modeling carbon storage profiles in temperate forest humic loamy soils of France. Soil Sci. 157, 185–192.

Bartholomeus, H., Kooistra, L., Stevens, A., van Leeuwen, M., van Wesemael, B., Ben-Dor, E., Tychon, B., 2011. Soil organic carbon mapping of partially vegetated agricultural fields with imaging spectroscopy. Int. J. Appl. Earth Obs. Geoinf. 13, 81–88.

Batjes, N.H., 1996. Total carbon and nitrogen in the soils of the world. Eur. J. Soil Sci. 47, 151–163.

Batjes, N.H., 2008a. ISRIC-WISE – Global Soil Profile Data. , (ver. 3.1) Wageningen.

Batjes, N.H., 2008b. Mapping soil carbon stocks of Central Africa using SOTER. Geoderma 146, 58–65.

Bellamy, P.H., Loveland, P.J., Bradley, R.I., Lark, R.M., Kirk, G.J.D., 2005. Carbon losses from all soils across England and Wales 1978–2003. Nature 437, 245–248.

Bellon-Maurel, V., McBratney, A., 2011. Near-infrared (NIR) and mid-infrared (MIR) spectroscopic techniques for assessing the amount of carbon stock in soils— Critical review and research perspectives. Soil. Biol. Biochem. 43, 1398–1410.

Bernoux, M., Arrouays, D., Cerri, C.C., Bourennane, H., 1998. Modeling vertical distribution of carbon in oxisols of the Western Brazilian Amazon (Rondonia). Soil Sci. 163, 941–951.

Bernoux, M., Carvalho, M.D.C.S., Volkoff, B., Cerri, C.C., 2002. Brazil's soil carbon stocks. Soil. Sci. Soc. Am. J. 66, 888–896.

Bhattacharyya, T., Pal, D.K., Easter, M., Batjes, N.H., Milne, E., Gajbhiye, K.S., Chandran, P., Ray, S.K., Mandal, C., Paustian, K., Williams, S., Killian, K., Coleman, K., Falloon, P., Powlson, D.S., 2007. Modelled soil organic carbon stocks and changes in the Indo-Gangetic plains, India from 1980 to 2030. Agric. Ecosyst. Environ. 122, 84–94.

Bishop, T.F.A., McBratney, A.B., Laslett, G.M., 1999. Modeling soil attribute depth functions with equal-area quadratic smoothing splines. Geoderma 91, 27–45.

Bou Kheir, R., Greve, M.H., Bøcher, P.K., Greve, M.B., Larsen, R., McCloy, K., 2010. Predictive mapping of soil organic carbon in wet cultivated lands using classification-tree based models: the case study of Denmark. J. Environ. Manag. 91, 1150–1160.

Breidt, F.J., Hsu, N.J., Ogle, S., 2007. Semiparametric mixed models for increment-averaged data with application to carbon sequestration in agricultural soils. J. Am. Stat. Assoc. 102, 803–812.

Brungard, C.W., Boettinger, J.L., 2010. Conditioned Latin hypercube sampling: optimal sample size for digital soil mapping of arid rangelands in Utah, USA. In: Boettinger, J.L., Howell, D.W., Moore, A.C., Hartemink, A.E., Kienast-Brown, S. (Eds.), Digital Soil Mapping: Bridging Research, Environmental Application, and Operation, Springer, Berlin, pp. 67–75.

Brus, D.J., de Gruijter, J.J., 2011. Design-based generalized least squares estimation of status and trend of soil properties from monitoring data. Geoderma 164, 172–180.

Brus, D.J., Kempen, B., Heuvelink, G.B.M., 2011. Sampling for validation of digital soil maps. Eur. J. Soil Sci. 62, 394–407.

Bui, E., Henderson, B., Viergever, K., 2009. Using knowledge discovery with data mining from the Australian Soil Resource Information System database to inform soil carbon mapping in Australia. Global Biogeochem. Cycles 23.

Burnham, H.J., Sletten, R.S., 2010. Spatial distribution of soil organic carbon in northwest Greenland and underestimates of high Arctic carbon stores. Global Biogeochem. Cycles 24.

Carré, F., Jeannée, N., Casalegno, S., Lemarchand, O., Reuter, H.I., Montanarella, L., 2010. Mapping the CN ratio of the forest litters in Europe—Lessons for global digital soil mapping. Progress in Soil Science In: Boettinger, J.L., Howell, D.W., Moore, A.C., Hartemink, A.E., Kienast-Brown, S. (Eds.), Digital Soil Mapping, Springer, Netherlands, pp. 217–226.

Carré, F., McBratney, A.B., Mayr, T., Montanarella, L., 2007a. Digital soil assessments: beyond DSM. Geoderma 142, 69–79.

Carré, F., McBratney, A.B., Minasny, B., 2007b. Estimation and potential improvement of the quality of legacy soil samples for digital soil mapping. Geoderma 141, 1–14.

Cerri, C.E.P., Easter, M., Paustian, K., Killian, K., Coleman, K., Bernoux, M., Falloon, P., Powlson, D.S., Batjes, N.H., Milne, E., Cerri, C.C., 2007. Predicted soil organic carbon stocks and changes in the Brazilian Amazon between 2000 and 2030. Agric. Ecosyst. Environ. 122, 58–72.

Chen, F., Kissel, D.E., West, L.T., Adkins, W., 2000. Field-scale mapping of surface soil organic carbon using remotely sensed imagery. Soil. Sci. Soc. Am. J. 64, 746–753.

De Gruijter, J.J., Brus, D.J., Bierkens, M.F.P., Knotters, M., 2006. Sampling for Natural Resource Monitoring. Springer, Berlin 332 pp.

Dobermann, A., 2002. Book review: shifting ground—the changing agricultural soils of China and Indonesia: by P.H. Lindert. MIT Press, Cambridge. Geoderma 107, 143–145.

Ellert, B.H., Bettany, J.R., 1995. Calculation of organic matter and nutrients stored in soils under contrasting management regimes. Can. J. Soil Sci. 75, 529–538.

Fantappiè, M., L'Abate, G., Costantini, E.A.C. 2011. The influence of climate change on the soil organic carbon content in Italy from 1961 to 2008. Geomorphology, 135, 343–352.

Gessler, P.E., Chadwick, O.A., Chamran, F., Althouse, L., Holmes, K., 2000. Modeling soil–landscape and ecosystem properties using terrain attributes. Soil. Sci. Soc. Am. J. 64, 2046–2056.

Gifford, R.M., Roderick, M.L., 2003. Soil carbon stocks and bulk density: spatial or cumulative mass coordinates as a basis of expression? Global Change Biol. 9, 1507–1514.

Goidts, E., Van Wesemael, B., Crucifix, M., 2009. Magnitude and sources of uncertainties in soil organic carbon (SOC) stock assessments at various scales. Eur. J. Soil Sci. 60, 723–739.

Gomez, C., Rossel, R.A.V., McBratney, A.B., 2008. Soil organic carbon prediction by hyperspectral remote sensing and field vis–NIR spectroscopy: an Australian case study. Geoderma 146, 403–411.

Grimm, R., Behrens, T., Märker, M., Elsenbeer, H., 2008. Soil organic carbon concentrations and stocks on Barro Colorado Island—Digital soil mapping using random forests analysis. Geoderma 146, 102–113.

Grunwald, S., 2009. Multi-criteria characterization of recent digital soil mapping and modeling approaches. Geoderma 152, 195–207.

Grunwald, S., Thompson, J.A., Boettinger, J.L., 2011. Digital soil mapping and modeling at continental scales: finding solutions for global issues. Soil. Sci. Soc. Am. J. 75, 1201–1213.

Guo, L.B., Gifford, R.M., 2002. Soil carbon stocks and land use change: a meta analysis. Global Change Biol. 8, 345–360.

Hénin, S., Dupuis, M., 1945. Essai de bilan de la matière organique du sol. Annales Agronomiques 11, 17–29.

Henry, M., Valentini, R., Bernoux, M., 2009. Soil carbon stocks in ecoregions of Africa. Biogeosci. Discuss. 6, 797–823.

Hollis, J.M., Hannam, J., Bellamy, P.H., 2012. Empirically-derived pedotransfer functions for predicting bulk density in European soils. Eur. J. Soil Sci. 63, 96–109.

Huang, X., Senthilkumar, S., Kravchenko, A., Thelen, K., Qi, J., 2007. Total carbon mapping in glacial till soils using near-infrared spectroscopy, landsat imagery and topographical information. Geoderma 141, 34–42.

Huber, S., Bareth, G., Doluschitz, R., 2002. Integrating the Process-based Simulation Model DNDC into GIS. Environmental Communication in the Information Society – Proceedings of the 16th Conference, Vienna, Austria, pp. 649–654.

Jenny, H., 1980. The Soil Resource: Origin and Behavior. Ecological Studies No. 37, Springer, New York.

Jenny, H., Salem, A.E., Wallis, J.R., 1968. Interplay of soil organic matter and soil fertility with state factors and soil properties. Study Week on Organic Matter and Soil Fertility. Pontif. Acad. Sci. Ser. Varia, 32, 1–33.

Jobbagy, E.G., Jackson, R.B., 2000. The vertical distribution of soil organic carbon and its relation to climate and vegetation. Ecol. Appl. 10, 423–436.

Kempen, B., Brus, D.J., Stoorvogel, J.J., 2011. Three-dimensional mapping of soil organic matter content using soil type-specific depth functions. Geoderma 162, 107–123.

Kunkel, M.L., Flores, A.N., Smith, T.J., McNamara, J.P., Benner, S.G., 2011. A simplified approach for estimating soil carbon and nitrogen stocks in semi-arid complex terrain. Geoderma 165, 1–11.

Lagacherie, P., Bailly, J.S., Monestiez, P., Gomez, C., 2012. Using scattered hyperspectral imagery data to map the soil properties of a region. Eur. J. Soil Sci. 63, 110–119.

Lal, R., 2004. Soil carbon sequestration impacts on global climate change and food security. Science 304, 1623–1627.

Lee, J., Hopmans, J.W., Rolston, D.E., Baer, S.G., Six, J., 2009. Determining soil carbon stock changes: simple bulk density corrections fail. Agric. Ecosyst. Environ. 134, 251–256.

Lilja, H., Nevalainen, R., 2006. Developing a digital soil map for Finland. In: Lagacherie, P., McBratney, A.B., Voltz, M. (Eds.), Developments in Soil Science, Elsevier, Amsterdam, pp. 67–74.

Lindert, P.H., 2000. Shifting Ground, the Changing Agricultural Soils of China and Indonesia. MIT Press, Cambridge.

Madari, B.E., Reeves Iii, J.B., Machado, P.L.O.A., Guimarães, C.M., Torres, E., McCarty, G.W., 2006. Mid- and near-infrared spectroscopic assessment of soil compositional parameters and structural indices in two Ferralsols. Geoderma 136, 245–259.

Malone, B.P., McBratney, A.B., Minasny, B., 2011. Empirical estimates of uncertainty for mapping continuous depth functions of soil attributes. Geoderma 160, 614–626.

Malone, B.P., McBratney, A.B., Minasny, B., Laslett, G.M., 2009. Mapping continuous depth functions of soil carbon storage and available water capacity. Geoderma 154, 138–152.

Marchetti, A., Piccini, R., Francaviglia, R., Santucci, S., Chiuchiarelli, I., 2010. Estimating soil organic matter content by regression kriging. Progress in Soil Science 2. In: Boettinger, J.L., Howell, D.W., Moore, A.C., Hartemink, A.E., Kienast-Brown, S. (Eds.), Digital Soil Mapping. Bridging Research, Environmental Application, and Operation, Springer, Heidelberg, pp. 241–254.

Martin, M.P., Wattenbach, M., Smith, P., Meersmans, J., Jolivet, C., Boulonne, L., Arrouays, D., 2011. Spatial distribution of soil organic carbon stocks in France. Biogeosciences 8, 1053–1065.

McBratney, A.B., Mendonça Santos, M.L., Minasny, B., 2003. On digital soil mapping. Geoderma 117, 3–52.

McGarry, D., Malafant, K.W.J., 1987. The analysis of volume change in unconfined units of soil. Soil. Sci. Soc. Am. J. 51, 290–297.

McKenzie, N.J., Jacquier, D.W., Maschmedt, D.J., Griffin, E.A., Brough, D.M., 2005. The Australian Soil Resource Information System Technical Specifications. Version 1.5.

McKenzie, N.J., Ryan, P.J., 1999. Spatial prediction of soil properties using environmental correlation. Geoderma 89, 67–94.

Meersmans, J., De Ridder, F., Canters, F., De Baets, S., Van Molle, M., 2008. A multiple regression approach to assess the spatial distribution of soil organic carbon (SOC) at the regional scale (Flanders, Belgium). Geoderma 143, 1–13.

Meersmans, J., van Wesemael, B., De Ridder, F., Van Molle, M., 2009. Modelling the three-dimensional spatial distribution of soil organic carbon (SOC) at the regional scale (Flanders, Belgium). Geoderma 152, 43–52.

Meersmans, J., Van Wesemael, B., Goidts, E., Van Molle, M., De Baets, S., De Ridder, F., 2010. Spatial analysis of soil organic carbon evolution in Belgian croplands and grasslands, 1960–2006. Global Change Biol. 17, 466–479.

Mendonça-Santos, M.L., McBratney, A.B., Minasny, B., 2006. Soil prediction with spatially decomposed environmental factors. In: Lagacherie, P., McBratney, A.B., Voltz, M. (Eds.), Developments in Soil Science, Elsevier, pp. 269–278.

Mendonça Santos, M.L., Dart, R.O., Santos, H.G., Coelho, M.R., Berbara, R.L.L., Lumbreras, J.F., 2010. Digital soil mapping of topsoil organic carbon content of Rio de Janeiro state, Brazil. In: Boettinger, J.L., Howell, D.W., Moore, A.C., Hartemink, A.E., Kienast-Brown, S. (Eds.), Digital Soil Mapping. Bridging Research, Environmental Application, and Operation, Springer, Heidelberg, pp. 255–265.

Miklos, M., Short, M.G., McBratney, A.B., Minasny, B., 2010. Mapping and comparing the distribution of soil carbon under cropping and grazing management practices in Narrabri, north-west New South Wales. Aust. J. Soil Res. 48, 248–257.

Milne, E., Adamat, R.A., Batjes, N.H., Bernoux, M., Bhattacharyya, T., Cerri, C.C., Cerri, C.E.P., Coleman, K., Easter, M., Falloon, P., Feller, C., Gicheru, P., Kamoni, P., Killian, K., Pal, D.K., Paustian, K., Powlson, D.S., Rawajfih, Z., Sessay, M., Williams, S., Wokabi, S., 2007. National and sub-national assessments of soil organic carbon stocks and changes: the GEFSOC modelling system. Agric. Ecosyst. Environ. 122, 3–12.

Minasny, B., Hartemink, A.E., 2011. Predicting soil properties in the tropics. Earth Sci. Rev. 106, 52–62.

Minasny, B., McBratney, A.B., 2006. A conditioned Latin hypercube method for sampling in the presence of ancillary information. Comput. Geosci. 32, 1378–1388.

Minasny, B., McBratney, A.B., 2010. Methodologies for global soil mapping. In: Boettinger, J.L., Howell, D.W., Moore, A.C., Hartemink, A.E., Kienast-Brown, S. (Eds.), Digital Soil Mapping: Bridging Research, Environmental Application, and Operation, pp. 429–436.

Minasny, B., McBratney, A.B., Mendonça-Santos, M.L., Odeh, I.O.A., Guyon, B., 2006. Prediction and digital mapping of soil carbon storage in the Lower Namoi Valley. Aust. J. Soil Res. 44, 233–244.

Minasny, B., McBratney, A.B., Salvador-Blanes, S., 2008. Quantitative models for pedogenesis—A review. Geoderma 144, 140–157.

Minasny, B., Sulaeman, Y., McBratney, A.B., 2010. Is soil carbon disappearing? The dynamics of soil organic carbon in Java. Global Change Biol. 17, 1917–1924.

Mishra, U., Lal, R., Liu, D.S., Van Meirvenne, M., 2010. Predicting the spatial variation of the soil organic carbon pool at a regional scale. Soil. Sci. Soc. Am. J. 74, 906–914.

Mishra, U., Lal, R., Slater, B., Calhoun, F., Liu, D., Van Meirvenne, M., 2009. Predicting soil organic carbon stock using profile depth distribution functions and ordinary kriging. Soil. Sci. Soc. Am. J. 73, 614–621.

Mora-Vallejo, A., Claessens, L., Stoorvogel, J., Heuvelink, G.B.M., 2008. Small scale digital soil mapping in Southeastern Kenya. Catena 76, 44–53.

Moreira, C.S., Brunet, D., Verneyre, L., Sá, S.M.O., Galdos, M.V., Cerri, C.C., Bernoux, M., 2009. Near infrared spectroscopy for soil bulk density assessment. Eur. J. Soil Sci. 60, 785–791.

Morgan, C.L.S., Waiser, T.H., Brown, D.J., Hallmark, C.T., 2009. Simulated in situ characterization of soil organic and inorganic carbon with visible near-infrared diffuse reflectance spectroscopy. Geoderma 151, 249–256.

Mueller, T.G., Pierce, F.J., 2003. Soil carbon maps: enhancing spatial estimates with simple terrain attributes at multiple scales. Soil. Sci. Soc. Am. J. 67, 258–267.

Muñoz, J.D., Kravchenko, A., 2011. Soil carbon mapping using on-the-go near infrared spectroscopy, topography and aerial photographs. Geoderma 166, 102–110.

Nyssen, J., Temesgen, H., Lemenih, M., Zenebe, A., Haregeweyn, N., Haile, M., 2008. Spatial and temporal variation of soil organic carbon stocks in a lake retreat area of the Ethiopian Rift Valley. Geoderma 146, 261–268.

Ouerghemmi, W., Gomez, C., Naceur, S., Lagacherie, P., 2011. Applying blind source separation on hyperspectral data for clay content estimation over partially vegetated surfaces. Geoderma 163, 227–237.

Phachomphon, K., Dlamini, P., Chaplot, V., 2010. Estimating carbon stocks at a regional level using soil information and easily accessible auxiliary variables. Geoderma 155, 372–380.

Ponce-Hernandez, R., Marriott, F.H.C., Beckett, P.H.T., 1986. An improved method for reconstructing a soil profile from analyses of a small number of samples. J. Soil Sci. 37, 455–467.

Post, W.M., Emanuel, W.R., Zinke, P.J., Stangenberger, A.G., 1982. Soil carbon pools and world life zones. Nature 298, 156–159.

Powers, J.S., Corre, M.D., Twine, T.E., Veldkamp, E., 2011. Geographic bias of field observations of soil carbon stocks with tropical land-use changes precludes spatial extrapolation. Proc. Natl. Acad. Sci. U. S. A. 108, 6318–6322.

Rawlins, B.G., Henrys, P., Breward, N., Robinson, D.A., Keith, A.M., Garcia-Bajo, M., 2011. The importance of inorganic carbon in soil carbon databases and stock estimates: a case study from England. Soil Use Manage. 27, 312–320.

Rawlins, B.G., Marchant, B.P., Smyth, D., Scheib, C., Lark, R.M., Jordan, C., 2009. Airborne radiometric survey data and a DTM as covariates for regional scale mapping of soil organic carbon across Northern Ireland. Eur. J. Soil Sci. 60, 44–54.

Razakamanarivo, R.H., Grinand, C., Razafindrakoto, M.A., Bernoux, M., Albrecht, A., 2011. Mapping organic carbon stocks in eucalyptus plantations of the central highlands of Madagascar: a multiple regression approach. Geoderma 162, 335–346.

Reeves, J.B., 2010. Near-versus mid-infrared diffuse reflectance spectroscopy for soil analysis emphasizing carbon and laboratory versus on-site analysis: where are we and what needs to be done? Geoderma 158, 3–14.

Russell, J.S., Moore, A.W., 1968. Comparison of different depth weightings in the numerical analysis of anisotropic soil profile data. In: Proc. 9th Int. Cong. Soil Sci. 4, 205–213.

Ruesch, A., Gibbs, H.K., 2008. New IPCC Tier-1 Global Biomass Carbon Map for the Year 2000. Available online from the Carbon Dioxide Information Analysis Center Oak Ridge National Laboratory, Oak Ridge, Tennessee. http://cdiac.ornl.gov.

Saby, N.P.A., Arrouays, D., Antoni, V., Lemercier, B., Follain, S., Walter, C., Schvartz, C., 2008. Changes in soil organic carbon in a mountainous French region, 1990–2004. Soil Use Manage. 24, 254–262.

Scharlemann, J., Hiederer, R., Kapos, V., 2009. Global Map of Terrestrial Soil Organic Carbon Stocks. UNEP-WCMC & EU-JRC, Cambridge, UK.
Schlesinger, W.H., 1977. Carbon Balance in terrestrial Detritus. Annu. Rev. Ecol. Syst. 8, 51–81.
Schulp, C.J.E., Veldkamp, A., 2008. Long-term landscape—land use interactions as explaining factor for soil organic matter variability in Dutch agricultural landscapes. Geoderma 146, 457–465.
Schwartz, D., Namri, M., 2002. Mapping the total organic carbon in the soils of the Congo. Global Planet Change 33, 77–93.
Selige, T., Böhner, J., Schmidhalter, U., 2006. High resolution topsoil mapping using hyperspectral image and field data in multivariate regression modeling procedures. Geoderma 136, 235–244.
Simbahan, G.C., Dobermann, A., Goovaerts, P., Ping, J., Haddix, M.L., 2006. Fine-resolution mapping of soil organic carbon based on multivariate secondary data. Geoderma 132, 471–489.
Smiles, D.E., 2009. Quantifying carbon and sulphate loss in drained acid sulphate soils. Eur. J. Soil Sci. 60, 64–70.
Smiles, D.E., Rosenthal, M.J., 1968. The movement of water in swelling materials. Aust. J. Soil Res. 6, 237–248.
Sombroek, W.G., Nachtergaele, F.O., Hebel, A., 1993. Amounts, dynamics and sequestering of carbon in tropical and subtropical soils. Ambio 22, 417–426.
Stevens, A., Udelhoven, T., Denis, A., Tychon, B., Lioy, R., Hoffmann, L., van Wesemael, B., 2010. Measuring soil organic carbon in croplands at regional scale using airborne imaging spectroscopy. Geoderma 158, 32–45.
Stoorvogel, J.J., Kempen, B., Heuvelink, G.B.M., de Bruin, S., 2009. Implementation and evaluation of existing knowledge for digital soil mapping in Senegal. Geoderma 149, 161–170.
Sulaeman, Y., Minasny, B., McBratney, A.B., 2010. Using legacy data to map the dynamics of soil organic carbon in Java, the 4th global workshop on digital soil mapping, Rome.
Thompson, J.A., Kolka, R.K., 2005. Soil carbon storage estimation in a forested watershed using quantitative soil-landscape modeling. Soil. Sci. Soc. Am. J. 69, 1086–1093.
Tonitto, C., Li, C., Seidel, R., Drinkwater, L., 2010. Application of the DNDC model to the Rodale Institute Farming Systems Trial: challenges for the validation of drainage and nitrate leaching in agroecosystem models. Nutr. Cycl. Agroecosyst. 87, 483–494.
Tranter, G., Minasny, B., McBratney, A.B., Murphy, B., McKenzie, N.J., Grundy, M., Brough, D., 2007. Building and testing conceptual and empirical models for predicting soil bulk density. Soil Use Manage. 23, 437–443.
Triantafilis, J., Buchanan, S.M., 2010. Mapping the spatial distribution of subsurface saline material in the Darling River valley. J. Appl. Geophys. 70, 144–160.
Triantafilis, J., Lesch, S.M., La Lau, K., Buchanan, S.M., 2009. Field level digital soil mapping of cation exchange capacity using electromagnetic induction and a hierarchical spatial regression model. Aust. J. Soil Res. 47, 651–663.
Ungaro, F., Staffilani, F., Tarocco, P., 2010. Assessing and mapping topsoil organic carbon stock at regional scale: a scorpan kriging approach conditional on soil map delineations and land use. Land Degrad. Develop. 21, 565–581.
Vasques, G.M., Grunwald, S., Comerford, N.B., Sickman, J.O., 2010a. Regional modelling of soil carbon at multiple depths within a subtropical watershed. Geoderma 156, 326–336.
Vasques, G.M., Grunwald, S., Sickman, J.O., 2008. Comparison of multivariate methods for inferential modeling of soil carbon using visible/near-infrared spectra. Geoderma 146, 14–25.
Vasques, G.M., Grunwald, S., Sickman, J.O., Comerford, N.B., 2010b. Upscaling of dynamic soil organic carbon pools in a north-central Florida watershed. Soil. Sci. Soc. Am. J. 74, 870–879.

Viaud, V., Angers, D.A., Walter, C., 2010. Towards landscape-scale modeling of soil organic matter dynamics in agroecosystems. Soil. Sci. Soc. Am. J. 74, 1–14.

Walter, C., Lagacherie, P., Follain, S., 2006. Integrating pedological knowledge into digital soil mapping. In: Lagacherie, P., McBratney, A.B., Voltz, M. (Eds.), Developments in Soil Science, Elsevier, , pp. 281–615.

Walter, C., Rossel, R.A.V., McBratney, A.B., 2003. Spatio-temporal simulation of the field-scale evolution of organic carbon over the landscape. Soil. Sci. Soc. Am. J. 67, 1477–1486.

Walvoort, D.J.J., Brus, D.J., de Gruijter, J.J., 2010. An R package for spatial coverage sampling and random sampling from compact geographical strata by k-means. Comput. Geosci. 36, 1261–1267.

Webster, R., 1978. Mathematical treatment of soil information. Trans. Int. Congr. Soil Sci. 11th 3, 161–190.

Webster, R., Oliver, M.A., 2007. Geostatistics for Environmental Scientists. John Wiley & Sons, Chichester, England.

Wheeler, I., Minasny, B., McBratney, A.B., Bui, E., Wilford, J., and Lymburner, L. Three-dimensional spatial prediction of soil organic carbon for three contiguous bioregions in New South Wales, Australia. Eur. J. Soil Sci., in press.

Wiesmeier, M., Barthold, F., Blank, B., Kögel-Knabner, I., 2011. Digital mapping of soil organic matter stocks using random forest modeling in a semi-arid steppe ecosystem. Plant Soil 340, 7–24.

Wilford, J., 2011. A weathering intensity index for the Australian continent using airborne gamma-ray spectrometry and digital terrain analysis. Geoderma.

Wilford, J., Minty, B., 2006. Chapter 16 the use of airborne gamma-ray imagery for mapping soils and understanding landscape processes. In: Lagacherie, A.B.M.P., Voltz, M. (Eds.), Developments in Soil Science, Elsevier, pp. 207–610.

Yoo, K., Amundson, R., Heimsath, A.M., Dietrich, W.E., 2006. Spatial patterns of soil organic carbon on hillslopes: integrating geomorphic processes and the biological C cycle. Geoderma 130, 47–65.

Zhang, C., Tang, Y., Xu, X., Kiely, G., 2011. Towards spatial geochemical modelling: use of geographically weighted regression for mapping soil organic carbon contents in Ireland. Appl. Geochem. 26, 1239–1248.

Zhao, Y.-C., Shi, X.-Z., 2010. Spatial prediction and uncertainty assessment of soil organic carbon in Hebei province, China. In: Boettinger, J.L., Howell, D.W., Moore, A.C., Hartemink, A.E., Kienast-Brown, S. (Eds.), Digital Soil Mapping: Bridging Research, Environmental Application, and Operation, Progress in Soil Science, Springer, Netherlands, pp. 227–239.

Zinn, Y.L., Lal, R., Resck, D.V.S., 2005. Texture and organic carbon relations described by a profile pedotransfer function for Brazilian Cerrado soils. Geoderma 127, 168–173.